Journal of Medicinal Chemistry

Drug Annotation

Design and Discovery of N-(3-(2-(2-hydroxyethoxy)-6-morpholinopyridin-4-yl)-4-methylphenyl)-2-(trifluoromethyl)isonicotinamide (LXH254)- A selective, efficacious and well-tolerated RAF inhibitor targeting RAS mutant cancers: The path to the clinic

Savithri Ramurthy, Benjamin Robert Taft, Robert J. Aversa, Paul Barsanti, Matthew T Burger, Yan Lou, Gisele Nishiguchi, Alice Rico, Lina Setti, Aaron Smith, Sharadha Subramanian, Victoriano N. A. Tamez, Huw R. Tanner, Lifeng Wan, Cheng Hu, Brent A Appleton, Mulugeta Mamo, Laura Tandeske, John E. Tellew, Shenlin Huang, Qin Yue, Apurva Chaudhary, Hung Tian, Raman Iyer, A. Quamrul Hassan, Lesley A. Mathews Griner, Laura R. LaBonte, Vesselina G. Cooke, Anne Van-Abbema, Hanne Merritt, Kalyani Gampa, Fei Feng, Jing Yuan, Yuji Mishina, Yingyun Wang, jacob haling, Sepideh Vaziri, Mohammad Hekmatnejad, Valery Polyakov, Xu(Richard) zang, Vijay Sethuraman, Payman Amiri, Mallika Singh, William R Sellers, Emma Lees, Wenlin Shao, Michael P Dillon, and Darrin D. Stuart

J. Med. Chem., **Just Accepted Manuscript** • DOI: 10.1021/acs.jmedchem.9b00161 • Publication Date (Web): 06 May 2019

ACS Publications

is published by the American Chemical Society. 1155 Sixteenth Street N.W., Washington, DC 20036

Pharmacology
Griner, Lesley; Novartis
LaBonte, Laura; Novartis Institutes for BioMedical Research Inc, Oncology Medicinal Chemisttry
Cooke, Vesselina; Novartis
Van-Abbema, Anne; Novartis Institute for BioMedical Research, Global Discovery Chemistry
Merritt, Hanne; Novartis Institute for BioMedical Research, Global Discovery Chemistry
Gampa, Kalyani; Novartis
Feng, Fei; Novartis
Yuan, Jing; Novartis
Mishina, Yuji ; Novartis Institutes for BioMedical Research Inc
Wang, Yingyun; Novartis Institute of Biomedical research
haling, jacob; Genomics Institute of the Novartis Research Foundation
Vaziri, Sepideh; Genomics Institute of the Novartis Research Foundation, Medicinal Chemistry
Hekmatnejad, Mohammad; Novartis Institutes for BioMedical Research Emeryville, Biochemical Lead Discovery
Polyakov, Valery; Novartis, NIBR
zang, Xu(Richard); Novartis, NIBR
Sethuraman, Vijay; Novartis, NIBR
Amiri, Payman; Novartis Institute of Biomedical research
Singh, Mallika; Novartis Institute for BioMedical Research, Global Discovery Chemistry
Sellers, William; Novartis Institutes for BioMedical Research Inc
Lees, Emma; Novartis Institutes for BioMedical Research Inc
Shao, Wenlin; Astra Zeneca,
Dillon, Michael; Ideaya Biosciences ,
Stuart, Darrin; Novartis

Design and Discovery of N-(3-(2-(2-hydroxyethoxy)-6-morpholinopyridin-4-yl)-4-methylphenyl)-2-(trifluoromethyl)isonicotinamide (LXH254)- A selective, efficacious and well-tolerated RAF inhibitor targeting RAS mutant cancers: The path to the clinic

Savithri Ramurthy*[1], Benjamin R. Taft[1], Robert J. Aversa[2], Paul A. Barsanti[1], Matthew T. Burger[2], Yan Lou[1], Gisele A. Nishiguchi[2], Alice Rico[1], Lina Setti[1], Aaron Smith[1], Sharadha Subramanian[1], Victoriano Tamez[2], Huw Tanner[1], Lifeng Wan[1], Cheng Hu[1], Brent A. Appleton[1], Mulugeta Mamo[1], Laura Tandeske[5], John E. Tellew[3], Shenlin Huang[3], Qin Yue[1], Apurva Chaudhary[7], Hung Tian[6], Raman Iyer[6], A. Quamrul Hassan[4], Lesley A. Mathews Griner[4], Laura R. La Bonte[4], Vesselina G. Cooke[4], Anne Van Abbema[5], Hanne Merritt[5], Kalyani Gampa[4], Fei Feng[4], Jing Yuan[4], Yuji Mishina[4], Yingyun Wang[5], Jacob R. Haling[3], Sepideh Vaziri[3], Mohammad Hekmat-Nejad[5], Valery Polyakov[1], Richard Zang[1], Vijay Sethuraman[5], Payman Amiri[5], Mallika Singh[5], William, R. Sellers[4], Emma Lees[4], Wenlin Shao[4], Michael P. Dillon[2], Darrin D. Stuart[4]

1 Global Discovery Chemistry, Novartis Institutes for BioMedical Research, 5300 Chiron Way, Emeryville, California 94608, United States

2 Global Discovery Chemistry, Novartis Institutes for BioMedical Research, 250 Massachusetts Avenue, Cambridge, Massachusetts 02139, United States

3. Genomics Institute of the Novartis Research Foundation, 10675 John Hopkins Dr, San Diego, California 92121

4. Oncology, Novartis Institutes for BioMedical Research, 250 Massachusetts Avenue, Cambridge, Massachusetts 02139, United States

5. Oncology, Novartis Institutes for BioMedical Research, 5300 Chiron Way, Emeryville, California 94608, United States

6. Technical Research & Development, Global Drug Development, Novartis Pharmaceuticals Corp., One Health Plaza, East Hanover , New Jersey, 07936, USA

7. Process Research and Development, Chemical and Analytical Development, Novartis Institute for Biomedical Research, One Health Plaza, East Hanover, New Jersey 07936, U.S.A.

ABSTRACT

Direct pharmacological inhibition of RAS has remained elusive and efforts to target CRAF have been challenging due to the complex nature of RAF signaling, downstream of activated RAS and the poor overall kinase selectivity of putative RAF inhibitors. Herein, we describe **15** (LXH254)[1], a selective B/C RAF inhibitor, which was developed by focusing on drug-like properties and selectivity. Our previous tool compound **3** (RAF709), a was potent, selective, efficacious, and well-tolerated in preclinical models, but the high human intrinsic clearance precluded further development[2] and prompted further investigation of close analogs. A structure-based approach led to a pyridine series with an alcohol side-chain that could interact with the DFG loop and significantly improved cell potency. Further mitigation of human intrinsic clearance and TDI led to the discovery of **15**. Due to its excellent properties, it was progressed through toxicology studies and is being tested in phase 1 clinical trials.

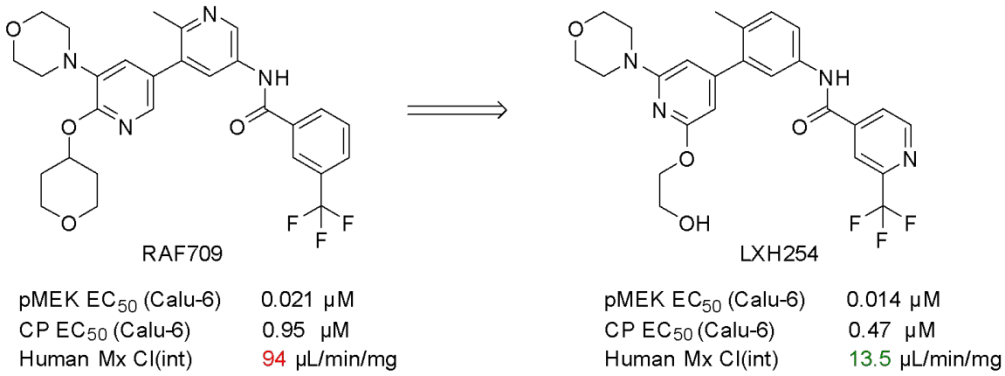

INTRODUCTION

The RAS-RAF-MEK-ERK or MAPK pathway plays a prominent role in transmitting signals from the cell membrane to the nucleus. Extracellular growth factors bind and activate cell surface receptor tyrosine kinases resulting in turnover of RAS-GDP (H-, N-, KRAS) to RAS-GTP in turn resulting in the engagement and activation of RAF kinases (A-, B-, CRAF), thus initiating the MAPK cascade. Just as this pathway is critical for growth, differentiation and homeostasis of normal tissues, it also plays a central role in the uncontrolled growth and invasiveness of human cancer. The RAS genes and BRAF are mutationally activated in approximately one-third of human tumors and genetic inactivation of CRAF prevents the

development of KRAS mutant tumors in genetically engineered mice. This dependence on signaling downstream of mutant RAS has provided therapeutic opportunities for targeting the RAF, MEK and ERK kinases which are eminently more druggable than RAS, with the possible exception of KRAS G12C for which covalent inhibitor approaches have been undertaken. [3-5]

Clinical proof-of-concept for targeting RAF has been demonstrated with drugs like dabrafenib (1) which potently inhibit $BRAF^{V600E}$ and provide significant tumor regression and increased survival in melanoma patients. However, the therapeutic potential of these drugs is restricted to tumors with $BRAF^{V600}$ mutations because in this context BRAF functions as a constitutively active monomer while in the RAS mutant setting, BRAF and CRAF function as dimers which are resistant to inhibition by these drugs.[6-9] Therefore, testing the therapeutic potential of targeting RAF downstream of mutant RAS will require compounds optimized to inhibit RAF dimers.[10] Furthermore, robust evaluation of this therapeutic hypothesis will require inhibitors with highly selective profiles so that the pharmacology is not compromised by off-target toxicity. For example, LY3009120 **(2)**, a pan-RAF inhibitor that effectively inhibits active RAF homo-and hetero-dimers has demonstrated preclinical activity in tumors with RAS mutations. However, **2** inhibits several other kinases, including those that have important roles in cancer such as Ephrin receptors, JNK and SRC family members which could also lead to off-target toxicities.[11] Such a profile could preclude dose-escalation to achieve potent RAF suppression in tumors and ultimately compromise the therapeutic utility of such a compound. Therefore, a highly selective RAF inhibitor will be invaluable in assessing the therapeutic utility in RAS mutant and atypical BRAF mutant tumors.

Chart 1

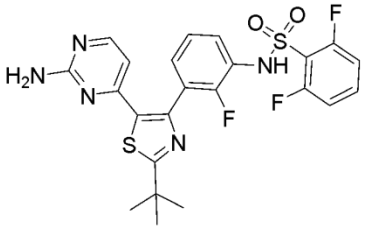

1. Dabrafenib

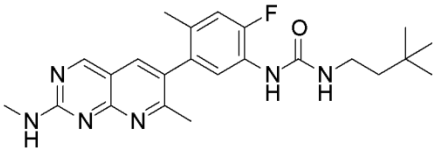

2. LY3009120

RESULTS AND DISCUSSION

Our previous disclosure[2] detailed the medicinal chemistry efforts to identify highly selective RAF inhibitors that potently suppress the RAF-MEK-ERK pathway in RAS/RAF mutant tumor cells without causing paradoxical activation. This led to the discovery of a key compound, **3**, which enabled numerous early pharmacology studies in RAS/RAF mutant xenograft models and validated the hypothesis that a wild-type B/CRAF inhibitor could prevent tumorigenesis in a RAS mutant setting with minimal paradoxical activation.

A key concern with **3** was the observed high clearance in human microsomes (Clint = 94 µL/min/mg), limiting the projected human exposure and preventing the compound from progressing as a clinical candidate. For this reason, we set out to understand the clearance mechanism and design analogs that could mitigate the high intrinsic human clearance. A cross species metabolism study was performed for **3** in rat, dog and human hepatocytes, where a number of metabolites were identified by LC/MS/MS (Figure 1). The major metabolites observed were an O-dealkylation product **(**M3) and tetrahydro-pyranyl ring oxidation (M4-M5) in all species. In addition, the amide hydrolysis product (M1 and M2) was found to be relatively abundant in rat hepatocytes compared to other species. No human unique metabolites were identified (**Figure 1**).

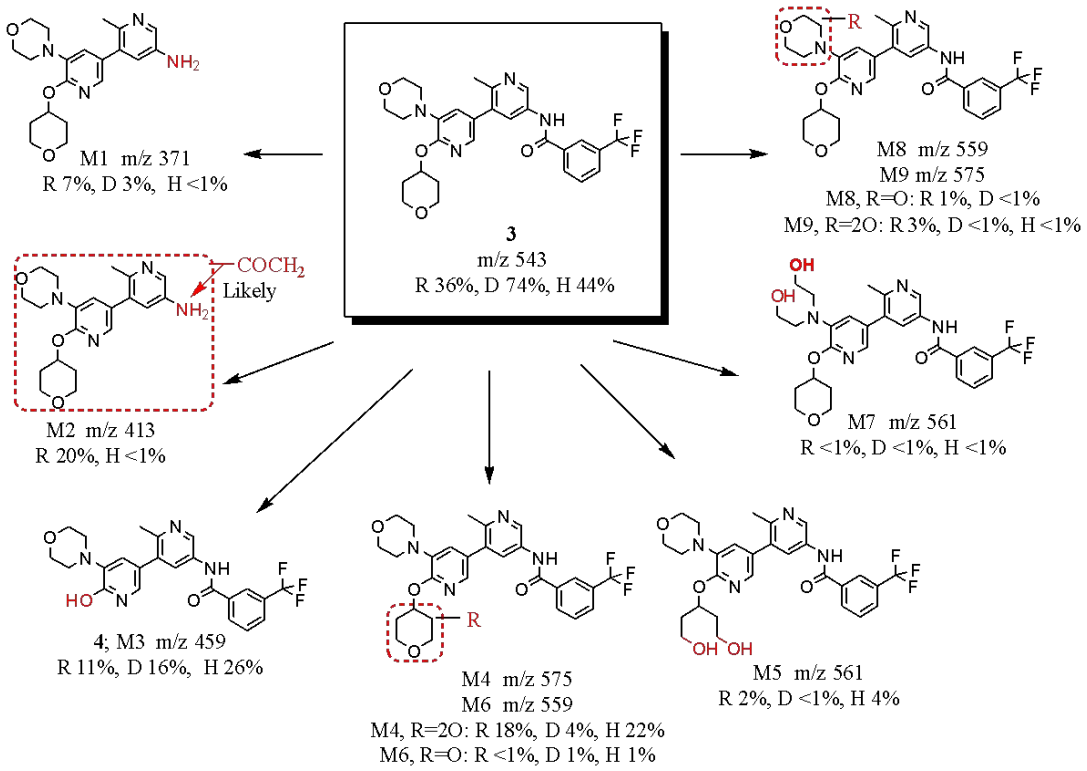

***Figure 1. Chemical structures of metabolites of 3 in* rat(R), dog (D), and human (H) hepatocyte (quantification based on UV response).**

With this knowledge, a focused set of THP analogs, in addition to the metabolite **4**, were synthesized and human microsomal clearance was determined (**Table 1)**. Not surprisingly, metabolite **4** showed 10-fold lower human Clint (9.4 vs 94), although when tested in a Calu-6 cellular proliferation (CP) assay, the compound was four-fold less potent (EC_{50} 3.9 μM vs 0.95 μM). This might be attributed to the significant increase in polarity and negative impact on cellular permeability as measured in the Caco-2 assay (AB/BA:0.3/43*)*. The fluoro-tetrahydropyranyl analog **5** retained good cellular potency and permeability, but this substitution had only a modest impact on the human Clint (65.5 vs 94). The methoxy-tetrahydropyranyl and deutero analogs (**6,7**) both showed good cellular potency, but neither had improved human Clint, and in fact, **6** had the highest measured Clint of all the analogs tested.

Table 1: Potency, ADME, and solubility data for tetrahydropyranyl analogues.

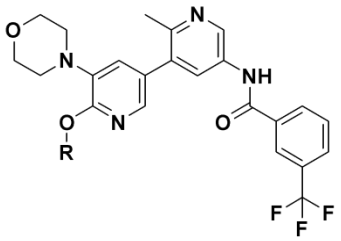

Cmpd	R	CRAF IC_{50} (μM)	pMEK Calu-6 EC_{50} (μM)	CP Calu-6 EC_{50} (μM)	Caco-2 Papp AB/BA (x10^{-6} cm/s)	Clint (human microsomal μL/min/mg)	Sol (μM)	cLogP
3	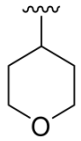	0.0003	0.021	0.95	15/13	94	200	4.2
4	H	0.0009	0.064	3.91	0.3/43	9.4	55	2.3
5	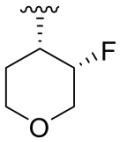	0.0003	0.005	0.34	16/20	65.5	25	4.5

6	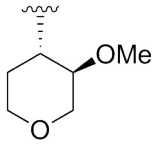	0.0017	0.021	1.76	NA	302	43	4.3
7	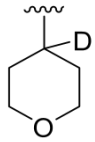	0.0004	0.006	0.40	NA	88	104	4.2

Table 2: Potency, ADME, and solubility data for CORE analogues.

Cmpd	R	CRAF IC_{50} (µM)	pMEK Calu-6 EC_{50} (µM)	CP Calu-6 EC_{50} (µM)	Caco-2 Papp AB/BA ($x10^{-6}$ cm/s)	Clint (human microsomal µL/min/mg)	Sol (µM)	cLogP
8	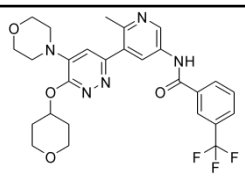	0.0004	0.008	0.88	4.4/51	7.7	59.6	3.3
9	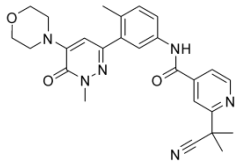	0.0011	0.052	1.35	6.3/49	15.5	33.9	1.5

Given the limited success in lowering human microsomal clearance by fine-tuning **3**, we hypothesized that increasing the polarity of the molecules might help mitigate oxidative metabolism. Analogs were synthesized and a representative set is shown in Table 2. Though polar analogs **8** and **9** had significantly lower human microsomal Clint compared to **3** and acceptable in vitro potency profile, these compounds had poor in vivo efficacy and a poor tolerability profile limiting their further progression.

We next re-evaluated the original pyrimidine hit scaffold[2] as this series had lower intrinsic clearance (43 μL/min/mg) while maintaining potent inhibition of pMEK and proliferation in Calu-6 cells. During this time, we considered many strategic options, one of which was to further optimize the cellular antiproliferative effect and pMEK EC_{50}. Although the protein-ligand interactions of our lead compounds were highly optimized, we re-examined early X-ray co-crystal structures to identify opportunities for growing into new vectors and gaining positive interactions with the protein. Careful examination of crystal structure of **10** (IC_{50}: 0.04 uM) with BRAF (Figure 2a) revealed no hinge binding, unlike typical type 2 B/C RAF kinase inhibitors which rely on interaction with the hinge. We attributed the potency to a very weak H-bonding interaction (N…O distance is slightly more than 3 Å) with the backbone carbonyl of F595 which could impact binding (**Figure 2a**), and is unique to the best of our knowledge, for Type 2 B/CRAF inhibitors. This prompted the team to search for compounds that are capable of interacting both with the hinge and with F595. Docking studies allowed us to hypothesize that compounds from our lead series could interact with F595 by extending an H-bond donor from the second carbon atom of the pyrimidine analog as with **11 (Table 3)**. This strategy led to the synthesis of many new analogs as represented in **Table 3** and we found that interaction with F595 led to compounds with significant improvement in cellular potency, although we do not have a clear mechanistic understanding for this observation. The F595 H-bonding interaction was best exemplified by **12**, which included an amino-ethanol sidechain at the second carbon of the pyrimidine ring and is a 'matched-pair' with **11**. As can be seen in the docking model of **12** (**Figure 2b**), the sidechain extends directly toward the F595 carbonyl without disrupting the conformation or other primary interactions. The oxygen atom of the sidechain is 2.9 angstroms away from the carbonyl of F595 and has an approach angle of 118°, strongly suggesting an H-bond with the protein. Compound **12**, showed a 33-fold improvement in cell activity compared to **11** (CP Calu-6 EC_{50} = 0.16 vs 5.28 μM), despite having slightly lower permeability (**Table 3**).

A

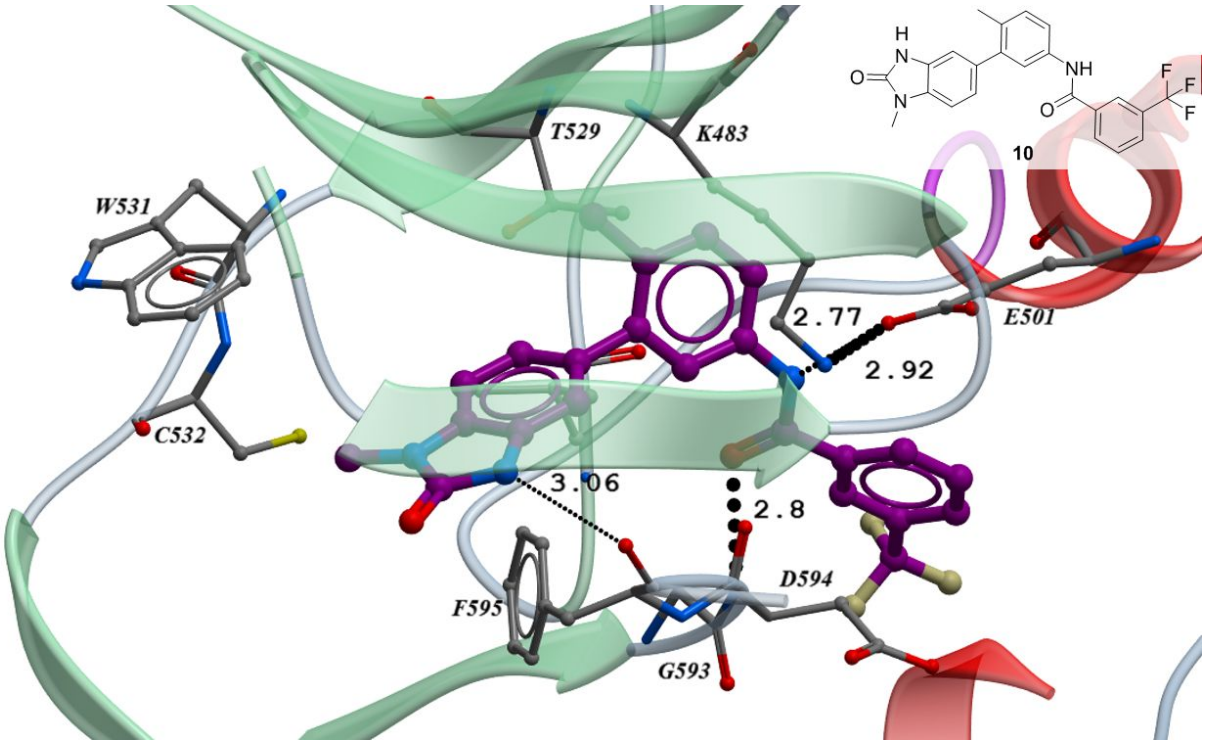

B

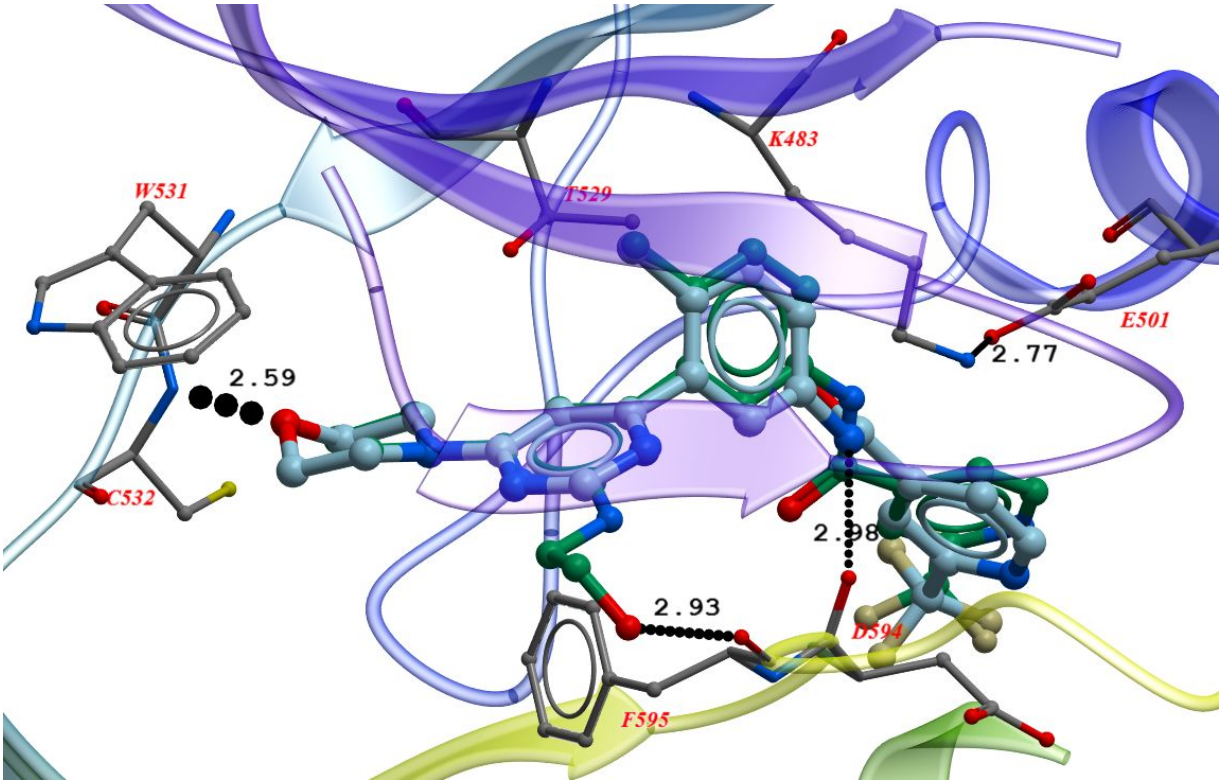

Figure 2: **A:** X-ray structure of **10** in BRAF (PDB 6N0Q)[12] **B**: Docking Models of **11** and **12** showing H-bond interaction with F595

Table 3: Potency, ADME, and TDI for pyridine/pyrimidine analogues.

Cmpd	R	CRAF IC_{50} (µM)	pMEK Calu-6 EC_{50} (µM)	CP Calu-6 EC_{50} (µM)	*Caco-2 Papp AB/BA (x10^{-6} cm/s)	Clint (human microsomal µL/min/mg)	**Sol (µM)	***cLogP	****TDI (k_{obs} min^{-1})
11	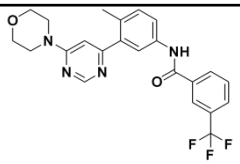	0.0001	--	5.28	19/41	43.3	13	4.0	
12	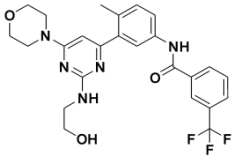	0.0002	0.061	0.16	8/30	48.0	2.1	4.1	
13	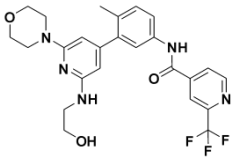	0.0006	0.008	0.51	5/53	20.5	36.3	3.2	0.035
14	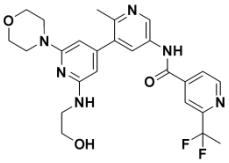	0.0007	0.027	6.22	3/34	10.4	730.2	2.1	0.035
15	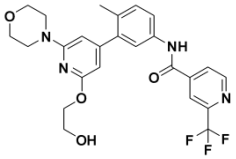	0.0002	0.014	0.47	9/19	13.5	20.0	3.5	0.01

*Forward and reverse flux were measured via transit across 21-day cultured Caco-2 monolayers at pH7.4 with quantification via LC/MS/MS. **Solubility (shake–flask assay) was measured with Cl-free PBS at pH 6.8. ***cLogP was calculated using Biobyte software.

****Time-dependent inhibition (TDI; k_{obs}) measured as described by Zimmerlin et. Al.,[13] Time dependent CYP3A4 inactivation screening assay (k_{obs}):Test compound at 10 µM is incubated with 0.5 mg/mL human liver microsome in

phosphate buffer containing 1 mM NADPH at 37 ˚C for 0, 5, 15, and 30 minutes. The incubation mixture is then diluted 20 times and incubated with CYP3A4 substrate midazolam (20 μM) at 37 ˚C for 6 minutes to determine residual CYP3A4 enzyme activity. The enzyme activity vs. incubation time is plotted to obtain the initial rate of decline which is defined as k_{obs} value.

Despite the improved cellular antiproliferative effect of **12,** the compound had low solubility, high lipophilicity and sub-optimal Clint (HLM). With this in mind, analogs with greater polarity in the aryl-rings were investigated, exemplified here by **13** and **14 (Table 3)**. When comparing **12, 13** and **14,** there was a clear trend that Clint (HLM) could be mitigated and solubility could be improved by increasing polarity albeit at the cost of reduced permeability and decreased cellular potency. In addition, during extended safety profiling of this chemical series, we observed a Cyp3A4 TDI signal which did not correlate with lipophilicity. It appeared that all pyridine analogs **13** and **14** bearing an amino-ethanol sidechain had a high risk for TDI (k_{obs} > 0.03) and this led us to hypothesize that the issue was associated with the electron-rich bis-amino pyridine functionality embedded in each compound. In an effort to make the rings electron deficient, the amino-ethanol side chain was changed to an ethylene glycol side chain (replacing nitrogen with oxygen). This strategy led to the discovery of **15** which maintained the critical F595 H-bond, but exhibited low risk for Cyp3A4 TDI (k_{obs} = 0.01) with the best balance of ADME properties and good cellular potency.

X-ray structure of 15. The X-ray co-crystal structure of **15** in BRAF, as illustrated in Figure 3, showed a binding mode similar to **3**.[2] As with **3**, the central toluyl tightly occupies a narrow hydrophobic pocket formed by a number of the sidechains including K483 and the gatekeeper residue T529. The CF_3 pyridyl moiety occupies the hydrophobic pocket formed by rotation of the DFG group, i.e. DFG-out, similar to the structure of compound **3** and other Type 2 kinase inhibitors.[14] The biggest difference with previously known structures was that the -hydroxyl of the glycolic moiety of **15** formed a strong hydrogen bond to the carbonyl of F595 manifested by 2.6 angstroms distance between the oxygen atoms and an approach angle of 120˚. All other hydrogen bonds seemed to be retained in the co-crystal, which might explain the strong potency of the compound.

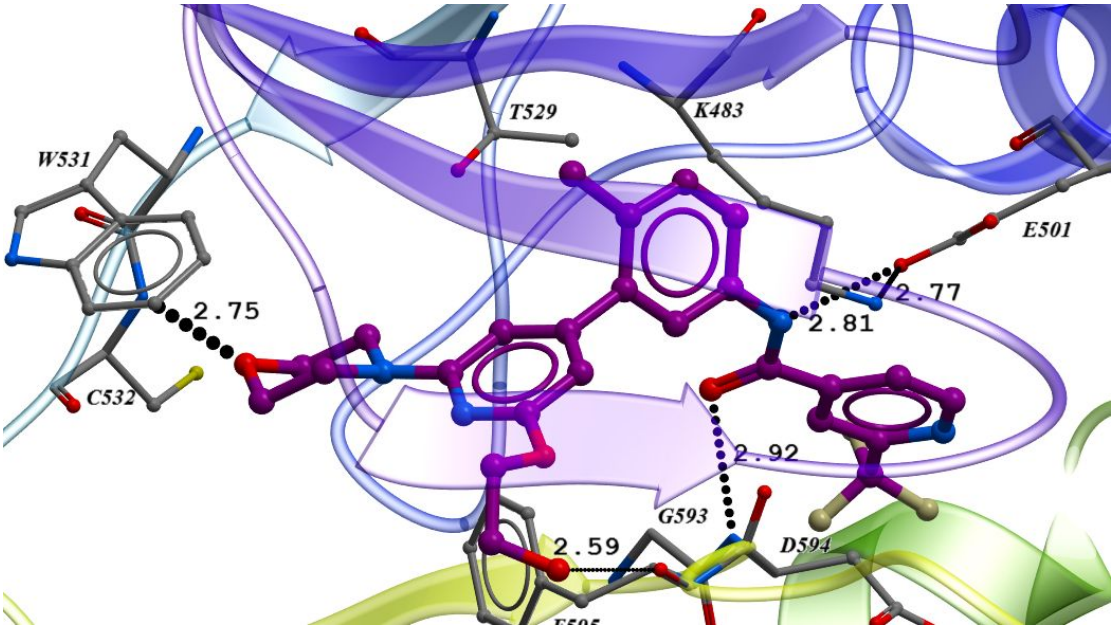

Figure 3: X-ray structure of **15** in BRAF (PDB 6N0P)[12]

***In vitro* profiling of 15[15].** The biochemical activity of **15** was further characterized against purified full-length BRAF where the IC_{50} was 0.0004 μM, and consistent with the potency against CRAF. Off-rate can be an important attribute of potency, affecting both the cellular activity in the face of feedback and the PK/PD relationship *in vivo.* The dissociation rate constant for **15** was measured using the rapid dilution method and full-length CRAF (with activating mutations Y340E/Y341E) kinase assay. The compound has a slow dissociation rate constant ($T_{1/2}$ > 6.5 hrs), as there was little recovery of enzyme activity after 6 hours of incubation in the kinase assay.

In cellular assays, the dose-response of **15** was measured using a pMEK assay in Calu-6 cells with an EC_{50} = 0.05 μM, minimal paradoxical activation (Figure 4) and inhibition of proliferation with EC_{50} = 0.28 μM. These data are clearly distinct from Compound **1** which demonstrated clear paradoxical activation in the pMEK assay (Figure 4) with maximum activity at 3 μM and no resultant inhibition up to the highest concentration tested (24 μM).

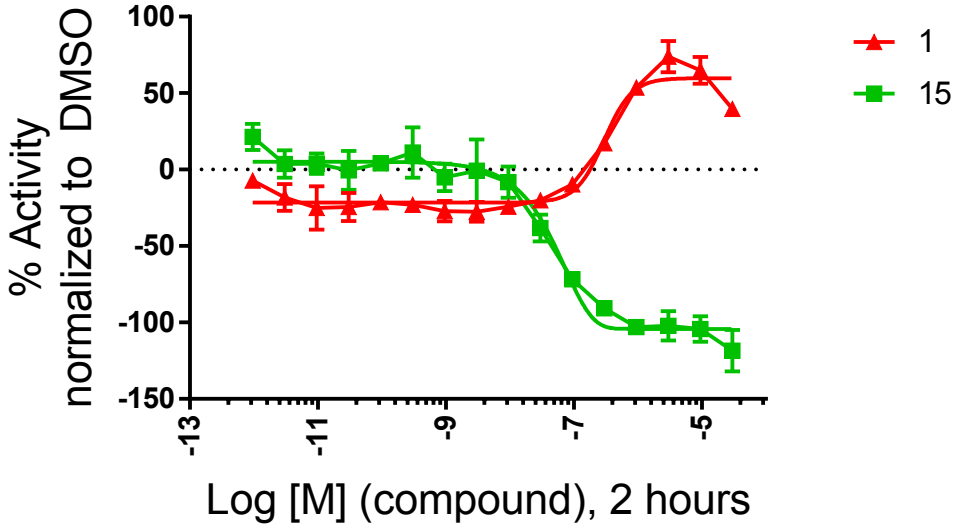

Figure 4: pMEK activity in Calu-6 cells of **15** vs **1**

The ability of **15** to stabilize RAF dimerization was measured using the CRAF:BRAF NanoBiT™ luciferase complementation assay (Promega). Consistent with most other RAF inhibitors[11,16] **15** stabilized BRAF-CRAF dimers with an EC_{50} = 0.16 μM (Figure **5**), while **1** yielded no significant effect on RAF dimerization as reported previously. Additional supporting data was revealed in the X-ray crystal structure of **15** (Figure 3), where each BRAF protomer in the dimer structure is occupied with compound. This also demonstrated that (at least under the conditions of crystallization), binding of **15** to one protomer did not preclude binding to the other protomer in the dimer structure. Altogether, these data demonstrate that **15** stabilizes RAF dimers but is relatively equipotent at inhibiting both protomers since it induces minimal paradoxical activation but effectively suppresses signaling.

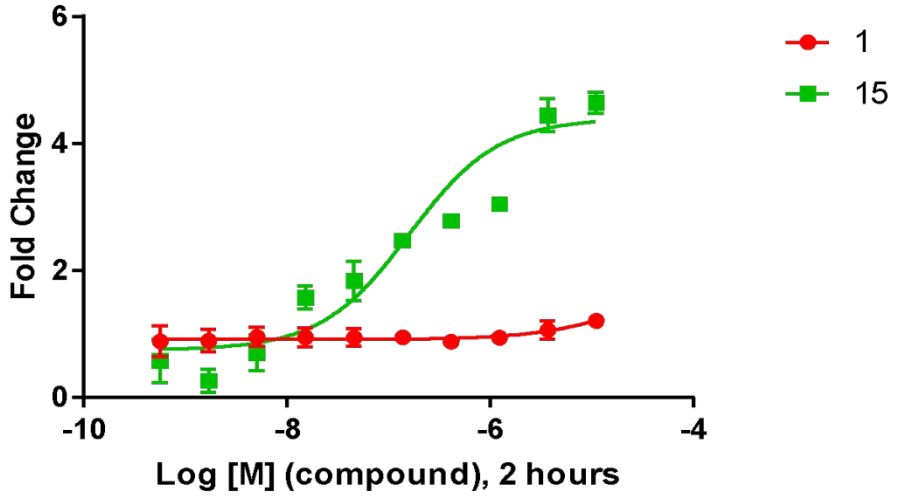

Figure 5. Effect of **1** and **15** on the RAF dimerization in HCT116 cells.

Kinase Selectivity of 15. Consistent with our early *in vivo* tool compound[2], **15** was found to be highly selective when evaluated using the KINOME*scan*™ screening platform. Of the 456 kinases tested, **15** showed a high level of selectivity (Figure 6) , demonstrating greater than 98% on-target binding to BRAF, BRAF^{V600E}, and CRAF at 1 μM and very few off-targets with DDR1 (>99%), DDR2 (84%), PDGFRb (>99%) the only kinases with binding >80% at 1 μM. The Kd values for these kinases was determined and were consistent with **15** being a potent inhibitor of BRAF (Kd = 1.3 nM) and CRAF (Kd = 3.6 nM) with similar potency against DDR1 (Kd = 1.8 nM) and less against DDR2 (Kd = 10 nM) and PDGFRb (Kd = 14 nM). To the best of our knowledge, this compound along with our earlier series, exhibit an extremely high level of kinase selectivity relative to other type 2 RAF inhibitors with a selectivity score of S(35) = 0.025. [17,18]

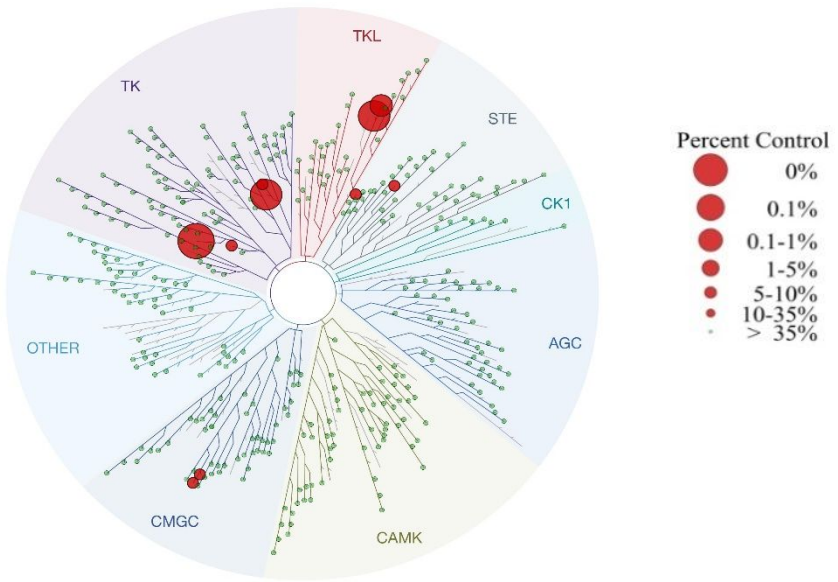

Figure 6: KINOME*scan* profile of **15**

Pharmacokinetics of 15. In pre-clinical pharmacokinetic experiments (Table 4), **15** had low to moderate clearance in mouse (19 mL/min/kg), rat (31 mL/min/kg) and dog (3.5 mL/min/kg). Cmax in mouse (1.6 μM), rat (0.5 μM) and dog (0.4 μM) reached pharmacologically active concentrations and acceptable oral availability was observed in mouse (65%), rat (38%) and dog (79%).

Table 4: PK profile of 15 across species

Species	Dose (*i.v./p.o*, mg/kg)	C_{max} (*p.o.*, μM)	AUC_{inf} (*p.o.*, ⌈M*hr)	Cl (mL/min/kg)	Vss (L/kg)	F(*po)* (%)
Mouse	2 / 4	1.6	4.3	19	2.1	65
Rat	2 / 4	0.5	1.8	31	5.4	38
Dog	0.2 / 0.4	0.4	3.1	3.5	1.7	79

*: formulation (*i.v./p.o)*: 25%PEG300 + 5%Solutol

PK/PD of 15. The PK/PD/efficacy relationship of **15** was examined in nude rats bearing Calu-6 ($KRAS^{Q61K}$) human NSCLC xenograft tumors. The plasma exposure and pMEK levels in tumor tissue were determined following a single oral administration of **15** across a dose range of 15, 35, 75, or 150 mg/kg. For each treatment group, tumor and blood samples were collected at 1, 4, 7, 24, and 48 hours post-dose. The effect of **15** on pMEK levels in the tumor was determined using an MSD immunoassay. The free plasma exposures of **15** were shown to be dose-proportional, corresponding with dose-dependent reductions in pMEK levels in tumors (Figure 7). At the higher dose level of 150 mg/kg, free plasma concentrations of **15** were maintained above the *in vitro* cellular pMEK IC_{50} value in Calu-6 for at least 24 hours, correlating with a sustained *in vivo* pMEK target inhibition of ~70% for the same duration.

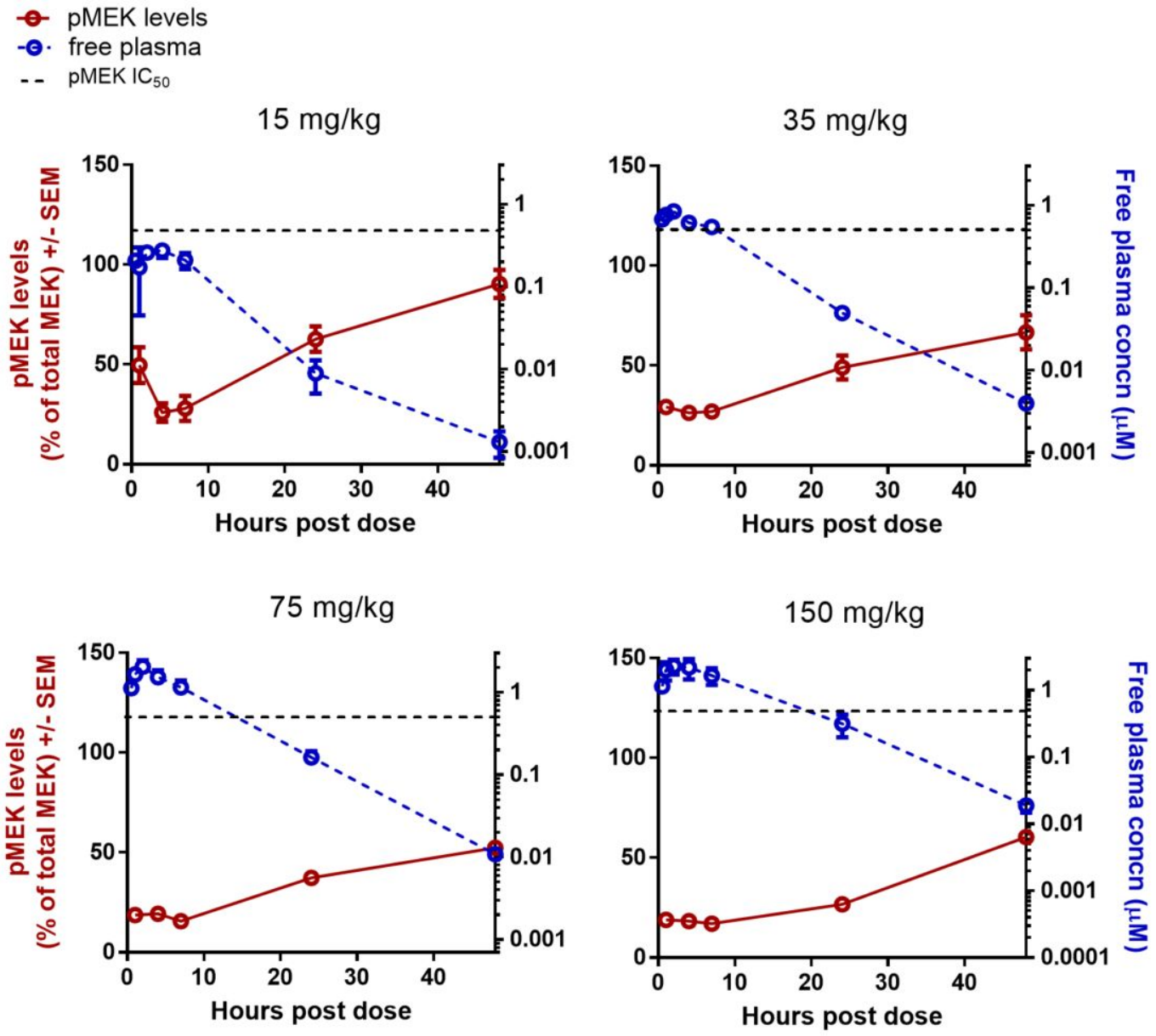

Figure 7 PK/PD analysis of **15** in the human Calu-6 NSCLC xenograft in rats. Percent pMEK levels (left axis), and free exposure (right axis) following a single dose of **15**, at time points indicated, in Calu-6 tumor bearing rats.

Efficacy and tolerability of 15 in the Calu-6 xenograft model. The antitumor efficacy and tolerability of **15** were determined in the Calu-6 xenograft nude rat model. Rats were treated with vehicle or **15** at 15, 35, 75 or 150 mg/kg p.o. daily beginning 13 days after tumor implantation and continued until day 31. The anti-tumor activity was determined by assessing %T/C or % regression on day 31 post-implant (18 days of treatment). Treatment with **15** resulted in dose-dependent anti-tumor activity with 15 mg/kg achieving 29% T/C. Treatment with 35 mg/kg resulted in tumor stasis

(%T/C=9%) and both 75 mg/kg and 150 mg/kg resulted in mean tumor regression of 21% and 56 % respectively (Figure 8a). All doses were well-tolerated with no significant body weight loss and no signs of toxicity or mortality (Figure 8b). Following the last dose of **15** in the efficacy study, plasma was collected, the concentration of **15** was measured and area under the curve (AUC) calculated for each dose (Table 5). **15** showed dose proportional plasma exposures and total plasma concentrations of AUC_{0-24}=104510 nM*h at steady state was associated with the lowest dose achieving tumor regression.

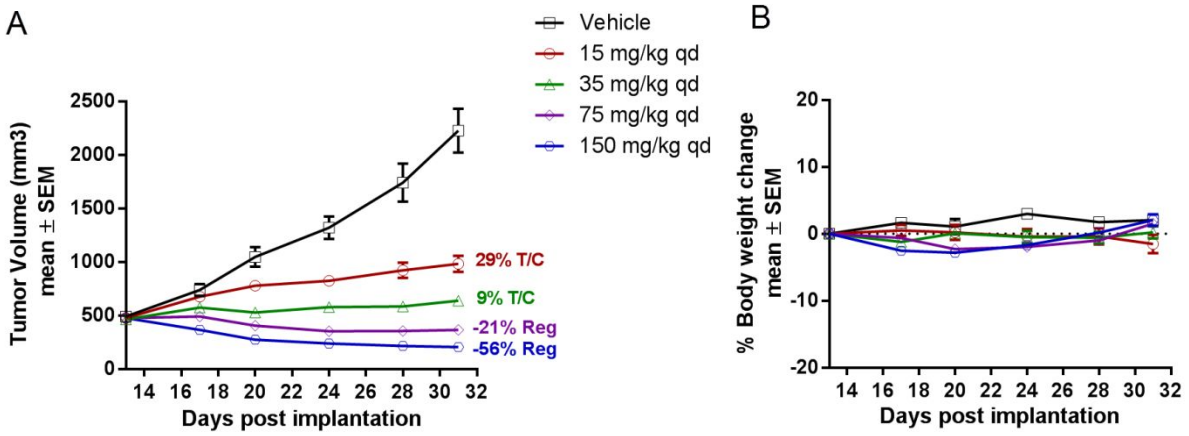

Figure 8 Efficacy of **15** in Calu-6 xenograft in rats. Tumor volumes (a) or percent body weight change from initial (b) treatment groups vs. vehicle control.

Table 5: Mean plasma pharmacokinetic parameters of 15 on day 31

	15mg/kg	**35mg/kg**	**75mg/kg**	**150mg/kg**
AUC (nM*h)	7913	25210	104510	216680
C_{max} (nM)	878	2347	8680	12671
T_{max} (h)	3	3	2	5.5
T_{last} (h)	24	24	24	24

With these encouraging rodent pharmacology activities and pharmacokinetic properties across species, **15** was profiled further with respect to developability and drug like properties. The melting point of **15** as a free base is 192 °C. Free form **15** has a log P>3, log D>4 (at pH 6.5) and pKa of 3.86. Its crystalline form solubility is 2 μg/mL. To increase the oral bioavailability, an amorphous solid dispersion formulation was developed. The solid dispersion was formed by combining drug and a stabilizing polymer in a suitable ratio along with other adjuvants under high thermomechanical stress followed by cooling and milling. The permeability (A-B) of **15** is medium to high at $9*10^{-6}$ cm/s. The stability in human plasma is high, with >90% intact after a 3 h incubation and the human plasma protein binding is 98%. In a manual patch clamp hERG assay, the compound exhibited a >10 uM IC_{50}.

On the basis of favorable cellular potency, kinase selectivity, preclinical pharmacology and physical properties, **15** was advanced into human clinical trials.

Chemistry:

Scheme 1. Synthesis for analogs **3-9**.

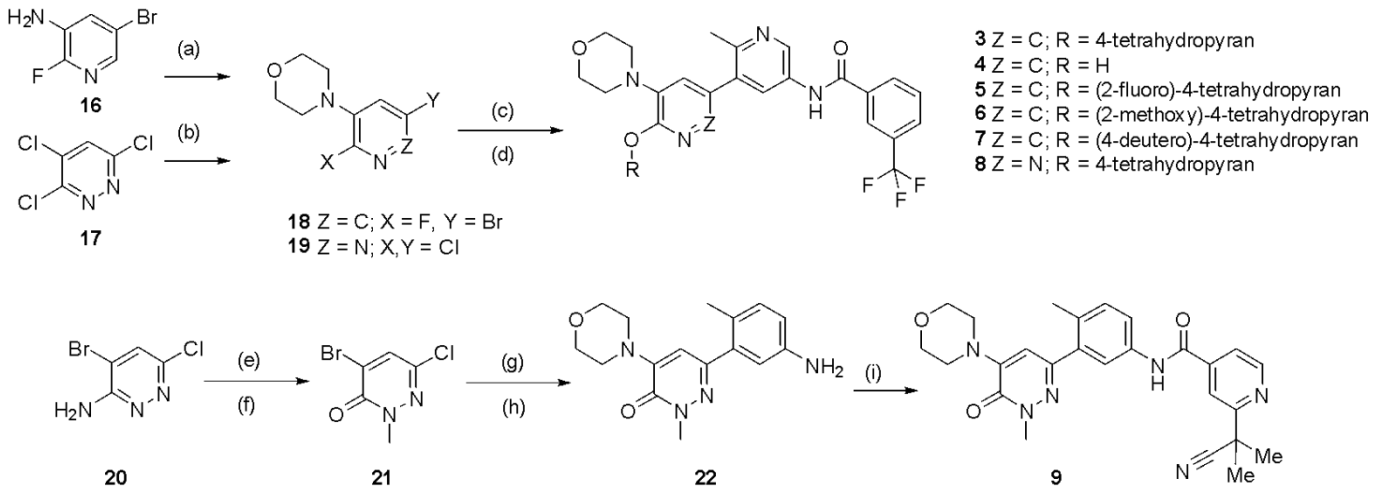

Reagents and Conditions. (a) $O(CH_2CH_2Br)_2$, NaH, DMF, 0 °C to RT. (b) morpholine, EtOH, RT. (c) N-(6-methyl-5-(4,4,5,5-tetramethyl-1,3,2-dioxaborolan-2-yl)pyridin-3-yl)-3-(trifluoromethyl)benzamide, $PdCl_2(dppf)\cdot CH_2Cl_2$, DME, 2M Na_2CO_3, 120 °C. (d) R-OH, NaH, dioxane or DMF, 90°C. (e) $NaNO_2$, H_2SO_4,

acetic acid, 0-25 °C, then water, 25 °C. (f) Cs_2CO_3, MeI, DMF. (g) morpholine, DMF, DIEA, 120 °C. (h) 4-methyl-3-(4,4,5,5-tetramethyl-1,3,2-dioxaborolan-2-yl)aniline, $PdCl_2(dppf)\cdot CH_2Cl_2$, DME, 2M Na_2CO_3, 120 °C. (i) Aryl-CO_2H, HATU, DIEA, DMF.

Compounds **3-9** were synthesized according to Scheme 1. In order to enable last step diversification and obtain final compounds exemplified in Table 1, intermediate **18** was synthesized from commercially available **16** via bis-alkylation with $O(CH_2CH_2Br)_2$. Subsequent Suzuki-Miyaura coupling reaction between **18** and N-(6-methyl-5-(4,4,5,5-tetramethyl-1,3,2-dioxaborolan-2-yl)pyridin-3-yl)-3-(trifluoromethyl)benzamide[2] yielded a fluoro-pyridine intermediate which was penultimate to the desired analogs. Treatment of this intermediate with the desired pre-formed alkoxide in dioxane or dimethylformamide allowed for isolation of final products (**3-7**) upon HPLC purification (Scheme 1). The pyridazine analog **8** was prepared in a similar fashion starting from commercial tri-chloride **17**. Compound **4** was prepared as reported in our last paper.[2] Compound **9** was prepared starting from amino-pyridazine **20** via hydrolysis of the corresponding diazonium species and subsequent N-methylation to give **21**. S_N2 addition of morpholine, followed by Suzuki-Miyaura coupling of 4-methyl-3-(4,4,5,5-tetramethyl-1,3,2-dioxaborolan-2-yl)aniline provided intermediate **22**, which was transformed to final compound **9** via typical amide coupling conditions. Scheme and synthesis of compound 10 is reported. [2]

Synthesis and experimental procedure for Compound **10** is reported in supporting information.

Scheme 2. Synthesis of analogs **12-15**.

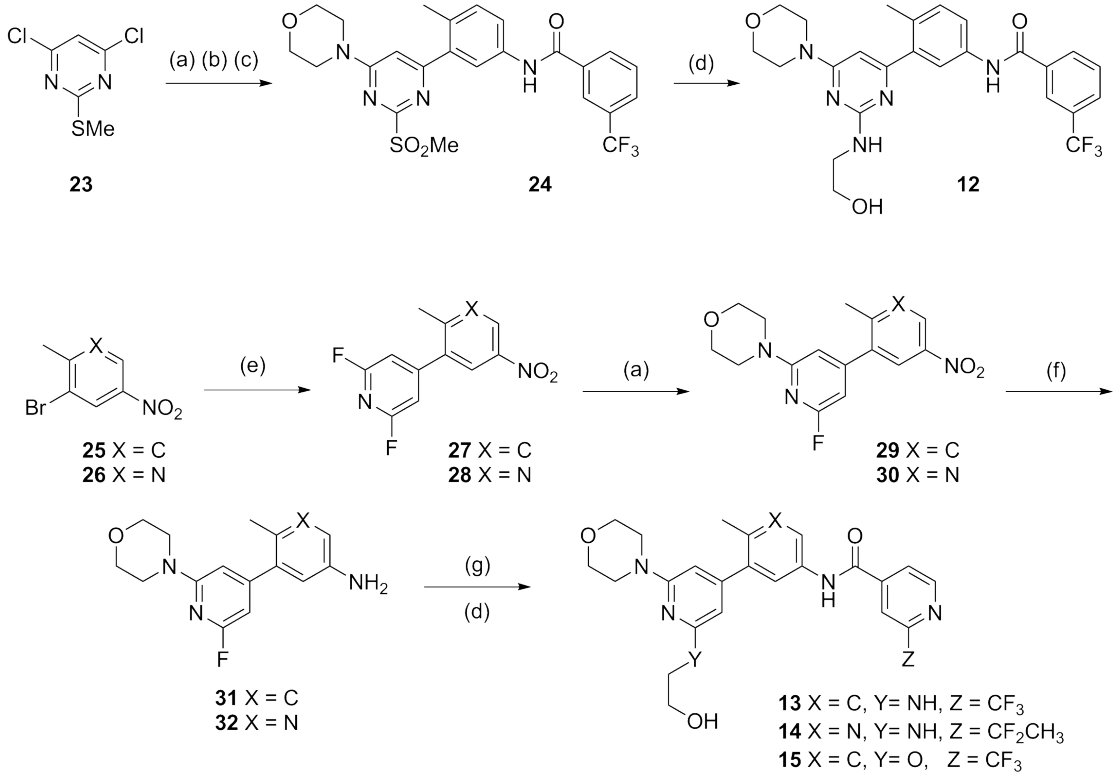

Reagents and Conditions. (a) morpholine, DIPEA, EtOH, RT or 55°C. (b) N-(4-methyl-3-(4,4,5,5-tetramethyl-1,3,2-dioxaborolan-2-yl)phenyl)-3-(trifluoromethyl)benzamide, $PdCl_2(dppf)\cdot CH_2Cl_2$, DME, 2M Na_2CO_3, 120 °C. (c) mCPBA, DCM, RT. (d) R-OH, NaH, dioxane, NMP, 150 °C or R-NH_2, K_2CO_3, DMSO, 55°C. (e) (2,6-difluoropyridin-4-yl)boronic acid, $PdCl_2(dppf)\cdot CH_2Cl_2$, DME, 2M Na_2CO_3, 60 °C. (f) H_2, 10% Pd/C, EtOH. (g) Aryl-CO_2H, HATU, DIPEA, DMF.

The synthesis of analogs **12-15** is outlined in Scheme 2. Compound **12** was synthesized starting from dichloropyrimidine **23** which was first subjected to S_N2 reaction with morpholine, followed by Suzuki-Miyaura coupling with N-(4-methyl-3-(4,4,5,5-tetramethyl-1,3,2-dioxaborolan-2-yl)phenyl)-3-(trifluoromethyl) benzamide, and then oxidation via mCPBA to yield intermediate **24**. Compound **24** was converted to analog **12** via S_N2 reaction with 2-aminoethanol.

Compounds **13-15** were prepared from commercial aryl- and pyridyl-nitro compounds **25** and **26**. Intermediates **29** and **30** were synthesized via Suzuki-Miyaura coupling reaction with (2,6-difluoropyridin-4-yl)boronic acid

followed by S_N2 reaction with morpholine. Hydrogenation then yielded intermediates **31** and **32**. Introduction of the side-chain groups at the 2-position of pyridine was performed through S_NAr reaction, and subsequent coupling of the anilines with carboxylic acids yielded **13-15** upon HPLC purification.

Scheme 3. Optimized synthesis of **15**.

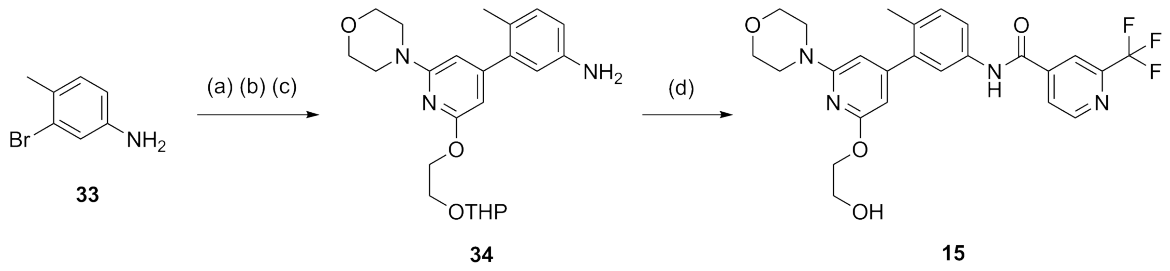

Reagents and Conditions. (a) (2,6-difluoropyridin-4-yl)boronic acid, Pd-XPhos precatalyst, 0.5 M K_3PO_4, THF, 35-60 °C, 64% yield. (b) morpholine, K_2CO_3, DMSO, 40°C, quantitative yield. (c) 2-((tetrahydro-2H-pyran-2-yl)oxy)ethanol, NaH, dioxane, 60-70 °C, 72% yield. (d) 2-(trifluoromethyl)-isonicotinic acid, EDC·HCl, HOAT, DIPEA, DMF, RT; then 2 M aqueous HCl, RT, 94% yield.

An optimized synthetic route for **15**, used to supply larger quantities of material for *in vivo* studies, is oulined in Scheme 3. A direct Suzuki-Miyaura coupling of 3-bromo-4-methylaniline **33** with the previously used boronic ester was possible using the Pd-XPhos precatalyst. Installation of the morpholine and ethylyene glycol moities were accomplished by successive S_NAr reactions, providing aniline **35**. Coupling of the aniline with the 2-(trifluoromethyl)-isonicotinic acid was followed by *in situ* acidic deprotection of the glycolic THP protecting group to afford **15** in high yield.

CONCLUSION:

Despite the clinical efficacy of RAF and MEK inhibitors in $BRAF^{V600}$ mutant melanoma[19-21] they are ineffective in RAS mutant tumors, leaving a significant unmet medical need. This class of RAF inhibitors approved for the treatment of $BRAF^{V600mut}$ melanoma, including **2**, induce paradoxical activation in BRAF wild-type cells and can induce growth of RAS^{mut} tumors. However, given the central role of CRAF in driving mutant KRAS-driven tumorigenesis, there remains a significant interest in developing RAF inhibitors that will be efficacious in RAS mutant tumors. Our work demonstrates that type 2 RAF inhibitors have the potential to be effective in RAS mutant tumors because they induce minimal paradoxical activation compared to RAF inhibitors with other binding modes (i.e. type 1 or type 1.5).[22] A previously disclosed *in vivo* tool **3**[2] gave the first evidence supporting this hypothesis, but could not be progressed further due to high intrinsic clearance in human microsomes. Due to limitations with the *in vivo* profile, we focused our efforts towards balancing physicochemical properties such as solubility and Cl(int) HLM with cellular potency, by tweaking the electronics of the ring system. This approach led to the identification of **15**, a compound shown to be highly kinase-selective and cellularly potent in a RAS mutant cell line (Calu-6) with minimal paradoxical activation. We believe this profile will enable the clinical development of the compound as a single-agent or in combination therapy. With the combination of potent in vitro activity and low to moderate CL, **15** demonstrates *in vivo* target modulation (pMEK), single agent antitumor activity in the Calu-6 rat xenograft model, and drug-like properties suitable for development. **15** was advanced into human studies and is currently being assessed in phase I trials.

EXPERIMENTAL SECTION:

General Methods. The compounds and/or intermediates were characterized by high performance liquid chromatography (HPLC) using a Waters Millennium chromatography system with a 2695 separation module (Milford, MA). The analytical columns were Alltima C-18 reversed phase, 4.6 mm x 50 mm, flow 2.5 mL/min, from Alltech (Deerfield, IL). A gradient elution was used, typically starting with 5% acetonitrile/95% water and

progressing to 100% acetonitrile over a period of 10 min. All solvents contained 0.1% trifluoroacetic acid (TFA). Compounds were detected by ultraviolet light (UV) absorption at either 220 or 254 nm. HPLC solvents were from Burdick and Jackson (Muskegan, MI) or Fisher Scientific (Pittsburgh, PA). Mass spectrometric analysis was performed on an LCMS instrument: a Waters system (Alliance HT HPLC and a Micromass ZQ mass spectrometer, Eclipse XDB-C18, 2.1 mm x 50 mm; solvent system, 5-95% acetonitrile in water with 0.1% TFA; flow rate 0.8 mL/min; molecular weight range 200-800; cone voltage 20 V; column temperature 40 °C). All masses were reported as those of the protonated parent ions. ^{1}H nuclear magnetic resonance (NMR) analyses described herein were performed on some of the compounds with a Varian 400-MR MHz NMR (Palo Alto, CA) spectrometer operating at a frequency of 399.89 MHz for ^{1}H or Bruker DRX-500 NMR spectrometer operating at a frequency of 500.13 MHz for ^{1}H. The spectral reference was either TMS or the known chemical shift of the solvent. The spectra were recorded at a temperature of 298 K. Preparative separations were carried out using a Teledyne ISCO chromatography system, or by HPLC using a Waters 2767 sample manager, C-18 reversed phase column, 30 x 50 mm, flow 75 mL/min. Typical solvents employed for the Teledyne ISCO chromatography system and were dichloromethane, methanol, ethyl acetate, and heptane. Typical solvents employed for the reverse phase HPLC were varying concentrations of acetonitrile and water with 0.1% trifluoroacetic acid. The purity of all compounds screened in the biological assays was examined by LC-MS analysis and were found to be ≥95%. Experimental details for the synthesis and characterization of compounds **3**, **4** and **11** are reported earlier.[2]

General procedure for S_NAr: To a mixture of sodium hydride, 60% in mineral oil (3-4 mmol) in dioxane or DMF at ambient temperature was added the appropriate alcohol (1.6 mmol). To the mixture was added N-(6'-fluoro-2-methyl-5'-morpholino-[3,3'-bipyridin]-5-yl)-3-(trifluoromethyl)benzamide[2] and the mixture was stirred for 2 h at 90 °C. The cooled reaction mixture was poured into water and extracted twice with EtOAc). The combined organics were washed with brine, dried over sodium sulfate, filtered, and concentrated. The mixture was purified by reverse phase HPLC to give the desired product.

General procedure for the amide formation reaction: To the appropriate aniline (0.050 mmol) in DMF (Volume: 0.75 mL) at RT were added HATU (0.050 mmol) and Huenig's Base (0.137 mmol) and the mixture

was stirred overnight. The reaction was filtered, dissolved in DMSO and then purified via reverse phase HPLC to give the desired product.

General Procedure for the Suzuki-Miyaura reaction: To the appropriate heteroaryl halide (0.10 mmol) and the appropriate boronic ester (0.12 mmol) in DME (1 mL) were added $PdCl_2(dppf)\cdot CH_2Cl_2$ adduct (0.010 mmol) and 2M aqueous sodium carbonate (0.50 mmol). The reaction mixture was irradiated at 120 °C in a Biotage Initiator microwave for 10-12 min. The cooled reaction mixture was diluted with 2:1 DCM:MeOH (15 mL) and filtered. The filtrate was concentrated and purified by reverse phase HPLC to give the desired product as its TFA salt.

N-(6'-(((3R,4S)-3-fluorotetrahydro-2H-pyran-4-yl)oxy)-2-methyl-5'-morpholino-[3,3'-bipyridin]-5-yl)-3-(trifluoromethyl)benzamide (5): To a stirred solution of 3-fluorodihydro-3-fluorodihydro-2H-pyran-4(3H)-one (100 mg, 0.847 mmol) in THF (5 mL) at -78 ^{o}C was added L-selectride (1 M in THF, 0.847 mL, 0.847 mmol) and the mixture was warmed to RT and stirred until no bubbling was observed. To the mixture was added 4-(5-bromo-2-fluoropyridin-3-yl)morpholine (221 mg, 0.847 mmol) and the reaction mixture was refluxed for 2h. The mixture was concentrated and purified by preparatory HPLC to give 4-(5-bromo-2-(((3R,4S)-3-fluorotetrahydro-2H-pyran-4-yl)oxy)pyridin-3-yl)morpholine (54 mg, 17.6% yield). LCMS m/z [M + H] =361/363, Rt = 0.88 min.

A mixture of 4-(5-bromo-2-(((3R,4S)-3-fluorotetrahydro-2H-pyran-4-yl)oxy)pyridin-3-yl)morpholine (54 mg, 0.15 mmol), N-(6-methyl-5-(4,4,5,5-tetramethyl-1,3,2-dioxaborolan-2-yl)pyridin-3-yl)-3-(trifluoromethyl)benzamide(60.7 mg, 0.149 mmol), 2M sodium carbonate solution (0.224 mL, 0.448 mmol) and $PdCl_2(dppf).CH_2Cl_2$ adduct (6 mg, 0.0007 mmol) in DME (2mL) was stirred at RT overnight. The reaction mixture was concentrated and purified by preparatory HPLC. The racemic mixture obtained was purified by chiral HPLC to give N-(6'-(((3R,4S)-3-fluorotetrahydro-2H-pyran-4-yl)oxy)-2-methyl-5'-morpholino-[3,3'-bipyridin]-5-yl)-3-(trifluoromethyl)benzamide (9.9 mg, 11.6% yield). LCMS m/z [M + H] =561.2, Rt = 0.78min. HRMS m/z (M^+ +1) calcd 561.2119, obsd 561.2115.

The following compounds were prepared by the above method starting from the appropriate heteroaryl-halide and the appropriate alcohol

N-(6'-(((3S,4S)-3-methoxytetrahydro-2H-pyran-4-yl)oxy)-2-methyl-5'-morpholino-[3,3'-bipyridin]-5-yl)-3-(trifluoromethyl)benzamide (6): Obtained in 2% yield. LCMS *m/z* [M + H^+] = 573.1, Rt = 0.76 min. HRMS m/z (M^++1) calcd 573.2319, obsd 573.2312.

N-(2-methyl-5'-morpholino-6'-((tetrahydro-2H-pyran-4-yl-4-d)oxy)-[3,3'-bipyridin]-5-yl)-3-(trifluoromethyl)benzamide (7): Obtained in 6% yield. LCMS *m/z* [M + H^+] = 544.1, Rt = 0.8 min. ^{1}H NMR (500 MHz, d_6-DMSO) δ ppm 1.72 (ddd, J = 12.8, 8.3, 4.0 Hz, 2H), 2.05 (dt, J = 9.1, 4.0 Hz, 2H), 3.11 (t, J = 4.5 Hz, 3H), 3.58 (ddd, J = 11.6, 8.2, 3.2 Hz, 2H), 3.77 (t, J = 4.5 Hz, 4H), 3.85 (dt, J = 10.9, 4.9 Hz, 2H), 7.29 (d, J = 2.1 Hz, 1H), 7.90 – 7.77 (m, 2H), 8.03 (d, J = 7.8 Hz, 1H), 8.26 (s, 1H), 8.31 (d, J = 7.9 Hz, 1H), 8.35 (s, 1H), 9.03 (d, J = 2.3 Hz, 1H), 10.93 (s, 1H). HRMS m/z (M+ + 1) calcd, obsd. HRMS m/z (M^+ +1) calcd 544.2276, obsd 544.2271.

N-(6-methyl-5-(5-morpholino-6-((tetrahydro-2H-pyran-4-yl)oxy)pyridazin-3-yl)pyridin-3-yl)-3-(trifluoromethyl)benzamide (8): Obtained in 43% yield. LCMS (m/z) (M+H) = 544.2, Rt = 0.75 min. LCMS (*m/z*) (M+H) = 472.3, Rt = 0.88 min. ^{1}H NMR (400 MHz, d_6-DMSO) δ ppm 1.03 (t, J=7.04 Hz, 1 H) 1.76 (dtd, J=12.62, 8.36, 8.36, 3.91 Hz, 2 H) 2.05 - 2.17 (m, 2 H) 3.32 - 3.38 (m, 4 H) 3.57 (ddd, J=11.44, 8.51, 3.13 Hz, 2 H) 3.69 - 3.77 (m, 4 H) 3.79 - 3.88 (m, 2 H) 5.51 (tt, J=8.02, 3.91 Hz, 1 H) 7.06 (s, 1 H) 7.79 (t, J=7.83 Hz, 1 H) 7.98 (d, J=7.83 Hz, 1 H) 8.20 (d, J=2.35 Hz, 1 H) 8.28 (d, J=7.83 Hz, 1 H) 8.32 (s, 1 H) 8.88 (d, J=2.74 Hz, 1 H) 10.68 (s, 1 H). HRMS m/z (M^++ 1) calcd, obsd. HRMS m/z (M+ + 1) calcd 544.2166, obsd 544.216.

2-(2-cyanopropan-2-yl)-N-(4-methyl-3-(1-methyl-5-morpholino-6-oxo-1,6-dihydropyridazin-3-yl)phenyl)isonicotinamide (9): To a cooled solution (0-5 °C) of sodium nitrite (1.350 g, 19.57 mmol) in

concentrated H_2SO_4 (10.1 mL, 189 mmol) was added 4-bromo-6-chloropyridazin-3-amine (1.7 g, 8.16 mmol) in acetic acid (33 mL). The reaction mixture was then stirred at 0 °C for 30 min before warming to RT. It was stirred for 1 h followed by the addition of water (51 mL), and stirred at RT for a further 4 h. The reaction mixture was then extracted with EtOAc, and the organic layer was dried over $MgSO_4$, filtered, and concentrated in vacuo to yield a brown oil which was further purified by flash column chromatography over silica gel, eluting with 100% heptanes to 80% EtOAc:heptanes to yield 4-bromo-6-chloropyridazin-3(2H)-one (1.42 g, 6.78 mmol) in 83% yield. LCMS m/z [M + H] =210.9/212.9, Rt = 0.42 min. ^{1}H NMR (400 MHz, d_6-DMSO) δ ppm 8.08 - 8.32 (m, 1 H) 13.25 - 13.71 (m, 1 H)

To a solution of 4-bromo-6-chloropyridazin-3(2H)-one (500 mg, 2.387 mmol) and Cs_2CO_3 (933 mg, 2.86 mmol) in DMF (33 mL) was added MeI (0.224 mL, 3.58 mmol) dropwise over 20 min. The resulting mixture was stirred for 3 h. The reaction mixture was then diluted with saturated aqueous NH_4Cl and then extracted twice with EtOAc. The combined organics were dried over $MgSO_4$, filtered and concentrated in vaccuo to yield a brown solid. The oil was further purified by flash column chromatography over silica gel, eluting with 100% heptanes to 80% EtOAc:heptanes to give 4-bromo-6-chloro-2-methylpyridazin-3(2H)-one as an off white solid (423 mg, 1.9 mmol) in 79% yield.

To a solution of 4-bromo-6-chloro-2-methylpyridazin-3(2H)-one (300 mg, 1.343 mmol) in DMF (4.5 mL) was added DIPEA (0.234 mL, 1.343 mmol) and morpholine (0.117 mL, 1.343 mmol) at RT. The resulting mixture was heated to 120 °C for 5 h. The reaction mixture was then diluted with water and extracted twice with EtOAc. The combined organics were dried over $MgSO_4$, filtered and concentrated in vacuo to give 6-chloro-2-methyl-4-morpholinopyridazin-3(2H)-one (300mg, 1.3 mmol) in 97% yield. LCMS m/z [M + H] =230/232, Rt = 0.64 min. The solid was utilized without further purification.

A solution of 6-chloro-2-methyl-4-morpholinopyridazin-3(2H)-one (100 mg, 0.435 mmol), Na_2CO_3 (302 mg, 2.85 mmol) and 4-methyl-3-(4,4,5,5-tetramethyl-1,3,2-dioxaborolan-2-yl)aniline (112 mg, 0.479 mmol) and $PdCl_2(dppf)\cdot CH_2Cl_2$ adduct (178 mg, 0.5 mmol) in DME (1.45 mL) and water (0.726 mL) was heated under

microwave irradiation for 40 min at 120 °C. The reaction mixture was then diluted with EtOAc and water, and the aqueous layer was then separated and extracted twice with EtOAc. The combined organics were dried over $MgSO_4$, filtered and concentrated in vacuo. The residue was purified by reverse phase HPLC to afford **9** as a brown solid in 24% yield. LCMS (m/z) (M+H) = 473.4, Rt = 0.84 min. ^{1}H NMR (500 MHz, d_6-DMSO) δ ppm 1.75 (s, 6 H) 2.29 (s, 3 H) 3.36 - 3.51 (m, 4 H) 3.57 - 3.76 (m, 7 H) 6.59 (s, 1 H) 7.30 (d, J=8.22 Hz, 1 H) 7.65-7.78 (m, 2 H) 7.85 (d, J=3.91 Hz, 1 H) 7.94 - 8.06 (m, 1 H) 8.79 (d, J=5.09 Hz, 1 H) 10.56 (s, 1 H). HRMS m/z (M^+ +1) calcd 473.2296, obsd 473.2291.

N-(4-methyl-3-(1-methyl-2-oxo-2,3-dihydro-1H-benzo[d]imidazol-5-yl)phenyl)-3-(trifluoromethyl)benzamide (10): NaH (60% in mineral oil, 1.64 g, 41.0 mmol) was added portionwise to a stirred solution of 1H-benzo[d]imidazol-2(3H)-one (5 g, 37.3 mmol) in dry DMF (100 mL) at RT that was maintained under an atmosphere of argon. After 75 min, a solution of di-tert-butyl dicarbonate (8.14 g, 37.3 mmol) in dry DMF (20 mL) was added dropwise, and the mixture was stirred at RT for 22 hours. The solvent was removed in vacuo, and the residue diluted with sat. NH_4Cl solution and extracted twice with EtOAc. The combined organics were dried over $MgSO_4$, filtered and concentrated in vacuo. The residue was purified by flash column chromatography over silica gel using a mixture of hexane and EtOAc (7:3) as eluent to furnish tert-butyl 2-oxo-2,3-dihydro-1H-benzo[d]imidazole-1-carboxylate (6.92 g, 29.5 mmol, 79 % yield) as a white solid. LCMS (m/z) (M+H) = 235.1, Rt = 0.76 min. ^{1}H NMR (400 MHz, $CDCl_3$) δ 1.70 (s, 9 H) 7.05 - 7.21 (m, 3 H) 7.67 - 7.84 (m, 1 H) 9.16 -9.30 (m, 1 H). ^{13}C NMR (101 MHz, $CDCl_3$) δ ppm 28.13 (s, 1 C) 76.70 (s, 1 C) 77.01 (s, 1 C) 77.33 (s, 1 C) 85.04 (s, 1 C) 109.90 (s, 1 C) 114.51 (s, 1 C) 122.12 (s, 1 C) 124.18 (s, 1 C) 126.91 (s, 1 C) 127.67 (s, 1 C) 148.61 (s, 1 C) 153.27 (s, 1 C).

Bromine (0.263 mL, 5.12 mmol) was added dropwise to a stirred solution of tert-butyl 2-oxo-2,3-dihydro-1H-benzo[d]imidazole-1-carboxylate (1 g, 4.27 mmol) and sodium acetate (0.366 g, 5.55 mmol) in acetic acid (13 mL) at RT. After 10 min, a precipitate formed and the mixture was continually stirred at RT for 2 h. The mixture was diluted with ice/water, and the yellow solid was filtered off and dried in air to give tert-butyl 6-bromo-2-oxo-

2,3-dihydro-1H-benzo[d]imidazole-1-carboxylate (1.2937 g, 4.13 mmol, 97 % yield) as a white solid. LCMS (m/z) (M+H) = 334.9/336.9, Rt = 0.93 min. ^{1}H NMR (400 MHz, $CDCl_3$) δ 1.69 (s, 10 H) 6.92 - 6.96 (m, 1 H) 7.28 - 7.33 (m, 1 H) 7.92 -8.00 (m, 1 H) 9.03 - 9.15 (m, 1 H). ^{13}C NMR (101 MHz, $CDCl_3$) δ ppm 28.13 (s, 1 C) 76.70 (s, 1 C) 77.01 (s, 1 C) 77.33 (s, 1 C)85.04 (s, 1 C) 109.90 (s, 1 C) 114.51 (s, 1 C) 122.12 (s, 1 C) 124.18 (s, 1 C) 126.91 (s, 1 C) 127.67 (s, 1 C)148.61 (s, 1 C) 153.27 (s, 1 C).

A mixture of tert-butyl 6-bromo-2-oxo-2,3-dihydro-1H-benzo[d]imidazole-1-carboxylate (300 mg, 0.958 mmol), MeI (0.090 mL, 1.437 mmol) and potassium carbonate (212 mg, 1.533 mmol) in acetonitrile (5 mL) was stirred at RT under argon for 16 h. As the reaction was incomplete by LCMS after this time, another 212 mg of potassium carbonate and 0.090 mL of methyl iodide were added into this mixture. It was stirred under argon at RT for another 5 hours. Upon completion of the reaction, EtOAc was added and the organic layer was washed with water, dried over sodium sulfate, filtered and concentrated. The crude residue was purified by flash column chromatography over silica gel, eluting with 50-100% ethyl aceatate in hexanes, to give tert-butyl 6-bromo-3-methyl-2-oxo-2,3-dihydro-1H-benzo[d]imidazole-1-carboxylate (120.6 mg, 0.369 mmol, 38.5 % yield). LCMS (m/z) (M+H) = 228.9/230.9.

Tert-butyl 6-bromo-3-methyl-2-oxo-2,3-dihydro-1H-benzo[d]imidazole-1-carboxylate (120.6 mg, 0.369 mmol) was dissolved in 2 mL of 1:1 TFA/DCM. The reaction mixture was stirred at RT for 30 minutes under argon. The solution was concentrated to remove most of solvent and TFA, basified to neutral with saturated aqueous sodium carbonate solution. The solution was extracted with ethyl acetate and the organic layer was separated, dried over sodium sulfate, filtered and concentrated. The crude residue was purified by flash column chromatography over silica gel to yield 5-bromo-1-methyl-1H-benzo[d]imidazol-2(3H)-one in quantitative yield.

A mixture of 5-bromo-1-methyl-1H-benzo[d]imidazol-2(3H)-one (70 mg, 0.308 mmol), 4-methyl-3-(4,4,5,5-tetramethyl-1,3,2-dioxaborolan-2-yl)aniline (216 mg, 0.925 mmol), and cesium carbonate (100 mg, 0.308 mmol) in dioxane (6 mL) and water (1.5 mL) was purged under argon for 3 minutes, $Pd(PPh_3)_4$ (35.6 mg, 0.031 mmol)

was added into the mixture and heated in microwave oven at 100 °C for 20 min. The reaction mixture was partitioned between ethyl acetate and water and the organic layer was separated, washed with water and brine, dried over sodium sulfate, filtered and concentrated. It was purified by flash column chromatography over silica gel eluting with 20% ethyl acetate in heptane to yield 5-(5-amino-2-methylphenyl)-1-methyl-1H-benzo[d]imidazol-2(3H)-one (60 mg, 0.237 mmol, 77%). LCMS (m/z) (M+H) = 254.1/230.9 Rt = 0.45 min.

To a mixture of 5-(5-amino-2-methylphenyl)-1-methyl-1H-benzo[d]imidazol-2(3H)-one (60 mg, 0.237 mmol) in ethyl acetate (2 mL) at RT were added DIPEA (0.084 mL, 0.474 mmol) and 3-(trifluoromethyl)benzoyl chloride (0.039 mL, 0.261 mmol) dropwise. The mixture was stirred at RT for 30 min. The reaction mixture was quenched with water and the reaction mixture was partitioned between ethyl acetate and water. The organic layer was separated, washed with water and brine, dried over sodium sulfate, filtered, and concentrated. The residue was purified by flash column chromatography over silica gel , eluting with 20% ethyl acetate in heptane, to yield N-(4-methyl-3-(1-methyl-2-oxo-2,3-dihydro-1H-benzo[d]imidazol-5-yl)phenyl)-3-(trifluoromethyl)benzamide (43.9 mg, 0.103 mmol, 43.6 % yield). LCMS (m/z) (M+H) = 425.6 Rt = 0.95 min. ^{1}H NMR (400 MHz, $CDCl_3$) δ ppm 2.19 (s, 3 H), 3.29 (s, 3 H), 6.89 (d, J=1.2 Hz, 1 H), 6.95 - 7.01 (m, 1 H), 7.12 (d, J=7.8 Hz, 1 H), 7.24 (d, J=8.2 Hz, 1 H), 7.62 (s,2 H), 7.71 - 7.79 (m, 1 H), 7.88 - 7.99 (m, 1 H), 8.16 - 8.33 (m, 2 H), 10.39 (s, 1 H), 10.81 - 10.93 (m, 1 H). HRMS m/z (M^+ +1) calcd 426.1424, obsd 426.1418.

N-(3-(2-((2-hydroxyethyl)amino)-6-morpholinopyrimidin-4-yl)-4-methylphenyl)-3-(trifluoromethyl)benzamide (12): To a solution of triethylamine (0.057 mL, 0.410 mmol) and 4,6-dichloro-2-(methylthio)pyrimidine (100 mg, 0.513 mmol) in ethanol (2.56 mL) at RT was added morpholine (0.046 mL, 0.513 mmol) in one portion. The resulting mixture was stirred at RT for 6 hrs. The precipitate formed was filtered and washed with ethanol to give 4-(6-chloro-2-(methylthio)pyrimidin-4-yl)morpholine (83 mg, 66%). LCMS (m/z) (M+H) = 246/247.9, Rt = 0.74 min**.**

The general procedure for the Suzuki-Miyaura reaction was followed for the next step utilizing the modified work-up: the reaction mixture was partitioned between water and EtOAc. The aqueous was further washed with

EtOAc (2 x 100mL). The combined organics were dried over $MgSO_4$, filtered, and concentrated. The residue was purified by flash column chromatography over silica gel, eluting with 0-60% EtOAc in heptanes, to provide N-(4-methyl-3-(2-(methylthio)-6-morpholinopyrimidin-4-yl)phenyl)-3-(trifluoromethyl)benzamide. Obtained in 60.4% yield. LCMS (m/z) (M+H) = 489.3, Rt = 0.8 min.

To a solution of N-(4-methyl-3-(2-(methylthio)-6-morpholinopyrimidin-4-yl)phenyl)-3-(trifluoromethyl)benzamide (1.20 g, 2.456 mmol) in DCM (33.0 mL) was added mCPBA (1.211 g, 5.40 mmol) portionwise. The reaction mixture was stirred at RT for 4 h, and then diluted with DCM (150 mL) and washed with 0.5 M Na_2CO_3. The resulting emulsion was filtered through a pad of Celite and the cake was washed with DCM. The organic layer was dried over $MgSO_4$, filtered and concentrated. The solid was triturated in DCM/heptanes and the product was filtered and dried to yield a light yellow solid to give N-(4-methyl-3-(2-(methylsulfonyl)-6-morpholinopyrimidin-4-yl)phenyl)-3-(trifluoromethyl)benzamide. LCMS (m/z) (M+H) = 521.2, Rt = 0.97 min.

To a solution of N-(4-methyl-3-(2-(methylsulfonyl)-6-morpholinopyrimidin-4-yl)phenyl)-3-(trifluoromethyl)benzamide (50 mg, 0.09 mmol) in THF (1 mL) were added 2-aminoethanol (11 mg, 0.19 mmol) and TEA (48.6 mg, 0.48 mmol) and the reaction mixture was heated to 120 °C in a microwave vial. The reaction mixture was concentrated, dissolved in DMSO and purified by preparatory HPLC to give N-(3-(2-((2-hydroxyethyl)amino)-6-morpholinopyrimidin-4-yl)-4-methylphenyl)-3-(trifluoromethyl)benzamide (11.2 mg, 0.017 mmol) in 18% yield. LCMS (m/z) (M+H) = 502.3, Rt = 0.76 min. ^{1}H NMR (500 MHz, CD_3OD) δ ppm 2.02 - 2.26 (m, 2 H) 2.38 (s, 3 H) 3.62 - 3.85 (m, 9 H) 4.04 (br. s., 2 H) 4.56 (br. s., 1 H) 6.52 (s, 1 H) 7.41 (d,J=8.22 Hz, 1 H) 7.66 (dd, J=8.22, 2.35 Hz, 1 H) 7.72 - 7.78 (m, 1 H) 7.92 (d, J=7.83 Hz, 1 H) 7.94 (d, J=1.96 Hz, 1 H) 8.21 (d, J=7.83 Hz, 1 H) 8.26 (s, 1 H). HRMS m/z (M^+ +1) calcd 502.2061, obsd 502.2055.

N-(3-(2-((2-hydroxyethyl)amino)-6-morpholinopyridin-4-yl)-4-methylphenyl)-2-(trifluoromethyl)isonicotinamide (13): To a mixture of 2-bromo-1-methyl-4-nitrobenzene (7 g, 32.5 mmol) and (2,6-difluoropyridin-4-yl)boronic acid (6.7 g, 42.1 mmol) were added DME (72 mL), 2 M aqueous sodium

carbonate solution (36 mL), and $PdCl_2(dppf)\cdot CH_2Cl_2$ adduct (1.02 g, 1.62 mmol) and the mixture was heated overnight at 60 °C. The reaction mixture was partitioned between water and ethyl acetate, the organic phase was dried with sodium sulfate, filtered and concentrated. The crude material was purified by flash column chromatography over silica gel, eluting with 0-100% ethyl acetate in heptanes, to provide 2,6-difluoro-4-(2-methyl-5-nitrophenyl)pyridine (4.24 g, 16.95 mmol, 52.3 % yield) as white crystalline solid. LCMS (m/z) (M+H) = 251, Rt = 0.94 min. ^{1}H NMR (400 MHz, $CDCl_3$) δ ppm 2.40 (s, 3 H) 6.82 (s, 2 H) 7.51 (d, J=8.22 Hz, 1 H) 8.11 (d, J=2.35 Hz, 1 H) 8.22 (dd, J=8.61, 2.35 Hz, 1 H).

To a solution of Huenig's Base (0.817 mL, 4.68 mmol) and 2,6-difluoro-4-(2-methyl-5-nitrophenyl)pyridine (390 mg, 1.559 mmol) in ethanol (5.2 mL) at RT was added morpholine (0.407 mL, 4.68 mmol) in one portion. The resulting mixture was then heated at 55 °C for 18 hours. Water was then added, and the resulting precipitate was filtered off to yield 4-(6-fluoro-4-(2-methyl-5-nitrophenyl)pyridin-2-yl)morpholine (500 mg, 1.5 mmol, 100 % yield). LCMS (m/z) (M+H)= 318.1, Rt = 1.04 min.

To a solution of 4-(6-fluoro-4-(2-methyl-5-nitrophenyl)pyridin-2-yl)morpholine (495 mg, 1.56 mmol) in ethanol (5.6 mL) was added 10% palladium on carbon, and the mixture was vacuum-degassed 3 times with hydrogen and stirred overnight under an atmosphere of hydrogen. The solution was filtered through Celite and concentrated to yield 3-(2-fluoro-6-morpholinopyridin-4-yl)-4-methylaniline (440 mg, 1.531 mmol, 98 % yield). LCMS (m/z) (M+H) =288, Rt = 0.63 min.

To a round-bottomed flask was added sodium hydride (69.6 mg, 1.740 mmol) and ethylene glycol (485 µL, 8.70 mmol) in dioxane (7.25 mL) and NMP (3.625 mL) and the mixture was stirred at RT for 20 min. At this time, a solution of 3-(2-fluoro-6-morpholinopyridin-4-yl)-4-methylaniline (250 mg, 0.870 mmol) in dioxane (1.0 mL) was added and the mixture was heated at 90 °C for 18 hours at which time LCMS showed ~40% conversion. The reaction mixture was further heated to 150 °C in the microwave for 30 min, The reaction mixture was quenched with saturated into $NaHCO_3$ solution and extracted twice with EtOAc. The combined organics were dried over $MgSO_4$, filtered, concentrated. The residue was purified purified by flash column chromatography over silica gel, eluting with 0-10% MeOH/DCM, to yield 2-((4-(5-amino-2-methylphenyl)-6-morpholinopyridin-2-

yl)oxy)ethanol (279 mg, 0.847 mmol, 97 % yield). LCMS (m/z) (M+H) =330.1, Rt = 0.53 min. ^{1}H NMR (400 MHz, CdCl3) δ ppm 2.26 (d, J = 4.9 Hz, 3H), 3.51 (q, J = 4.8 Hz, 4H), 3.79 (ddd, J = 6.7, 4.0, 1.8 Hz, 4H), 3.91 - 3.84 (m, 1H), 4.41 - 4.33 (m, 1H), 4.76 - 4.59 (m, 2H), 6.32 - 6.24 (m, 1H), 6.13 (dd, J = 28.4, 0.9 Hz, 1H), 7.33 - 7.25 (m, 1H), 7.68 - 7.56 (m, 2H), 8.14 - 8.07 (m, 1H), 8.31 - 8.26 (m, 1H), 8.93 - 8.86 (m, 1H).

Following the General procedure for the amide formation, **13** was obtained in 30% yield. LCMS (*m/z*) (M+H) = 502.1, Rt = 0.73 min. ^{1}H NMR (400 MHz, DMSO-*d6*) δ ppm 2.32 (s, 3 H) 3.52 (q, J=4.43 Hz, 6 H) 3.72 - 3.95 (m, 6 H) 6.21 (d, J=10.96 Hz, 1 H) 7.35 (d, J=8.22 Hz, 1 H)7.60 (dd, J=8.22, 1.96 Hz, 1 H) 7.77 (s, 1 H) 8.12 (d, J=4.70 Hz, 1 H) 8.29 (s, 1 H) 8.92 (d, J=5.09 Hz, 1 H). HRMS m/z (M^+ +1) calcd 502.2061, obsd 502.2055.

The following compounds were synthesized following similar procedures as compound **13** above:

2-(1,1-difluoroethyl)-N-(2'-((2-hydroxyethyl)amino)-2-methyl-6'-morpholino-[3,4'-bipyridin]-5-yl)isonicotinamide (14): Obtained in 63.2% yield. LCMS (m/z) (M+H) = 499.2, Rt = 0.53 min. ^{1}H NMR (500 MHz, Methanol-d4) δ ppm 2.07 (t, J=18.76 Hz, 3 H) 2.64 (s, 3 H) 3.52 - 3.59 (m, 6 H) 3.80 - 3.88 (m, 6 H) 6.20 - 6.28 (m, 1 H)8.03 (d, J=5.04 Hz, 1 H) 8.25 (s, 1 H) 8.43 (d, J=2.52 Hz, 1 H) 8.88 (d, J=4.73 Hz, 1 H) 9.09 (d, J=1.58 Hz, 1 H). HRMS m/z (M^+ +1) calcd 499.2264, obsd 499.2256.

N-(3-(2-(2-hydroxyethoxy)-6-morpholinopyridin-4-yl)-4-methylphenyl)-2-(trifluoromethyl)isonicotinamide (15): Obtained in 36% yield. LCMS (m/z) (M+H) = 503.1, Rt = 0.89 min. ^{1}H NMR (500 MHz, Methanol-d4) δ ppm 2.26 (d, J = 4.9 Hz, 3H), 3.51 (q, J = 4.8 Hz, 4H), 3.79 (ddd, J = 6.7, 4.0, 1.8 Hz, 4H), 3.91 – 3.84 (m, 1H), 4.41 – 4.33 (m, 1H), 4.76 – 4.59 (m, 2H), 6.13 (dd, J = 28.4, 0.9 Hz, 1H), 6.32 – 6.24 (m, 1H), 7.33 – 7.25 (m, 1H), 7.68 – 7.56 (m, 2H), 8.14 – 8.07 (m, 1H), 8.31 – 8.26 (m, 1H), 8.93 – 8.86 (m, 1H). HRMS m/z (M^+ +1) calcd 503.1906, obsd 503.1902.

Optimized synthesis of N-(3-(2-(2-hydroxyethoxy)-6-morpholinopyridin-4-yl)-4-methylphenyl)-2-(trifluoromethyl)isonicotinamide (15): 3-bromo-4-methylaniline (8.03 g, 43.1 mmol), (2,6-difluoropyridin-4-yl)boronic acid (10 g, 41.5 mmol), and Pd-XPhos precatalyst (0.163 g, 0.207 mmol) were stirred in a solution of THF (83 mL) under nitrogen. 0.5M potassium phosphate solution (166 mL) was added and the mixture was

heated overnight at 35 °C. More Pd-Xphos precatalyst (0.163 g, 0.207 mmol) was added, and the mixture was warmed to 60 °C for 18 hours. The mixture was carefully poured onto water and extracted three times with ethyl acetate. The combined organics were washed with water, dried over magnesium sulfate, filtered and concentrated. The crude material was purified purified by flash column chromatography over silica gel, eluting with 0-100% ethyl acetate in heptane, to give 3-(2,6-difluoropyridin-4-yl)-4-methylaniline (5.87 g, 26.7 mmol, 64 % yield). LCMS (m/z) (M+H) = 220.9, Rt = 0.54 min.

To a solution of 3-(2,6-difluoropyridin-4-yl)-4-methylaniline (5.87 g, 26.7 mmol) in DMSO (26.7 mL) was added morpholine (6.92 ml, 80 mmol) and potassium carbonate (7.37 g, 53.3 mmol). The mixture was heated at 40 °C for 3 hours, and upon cooling to RT, diluted with water and sodium bicarbonate and extracted three times with ethyl acetate. The combined organics were dried over $MgSO_4$, filtered and concentrated to give 3-(2-fluoro-6-morpholinopyridin-4-yl)-4-methylaniline (7.66 g, 26.7 mmol, quantitative yield). LCMS (m/z) (M+H)= 288.0, Rt = 0.60 min.

To a solution of 3-(2-fluoro-6-morpholinopyridin-4-yl)-4-methylaniline (7.66 g, 26.7 mmol) in dioxane (132 mL) was added 2-((tetrahydro-2H-pyran-2-yl)oxy)ethanol (7.18 mL, 52.9 mmol). Sodium hydride (60% dispersion, 2.116 g, 52.9 mmol) was added carefully and the reaction was stirred at RT for 30 minutes, then warmed to 60 °C for 2 hours. At this point, about 75% conversion to product was observed by LCMS, so the mixture was heated to 70 °C for an additional one hour. The reaction was cooled to RT, quenched with aqueous sodium bicarbonate, and extracted three times ethyl acetate. The combined organics were dried over magnesuim sulfate, filtered and concentrated. The crude material was purified by flash column chromatography over silica gel, eluting with 0-5% methanol in DCM and then 0-100% ethyl acetate in heptanes, to give 4-methyl-3-(2-morpholino-6-(2-((tetrahydro-2H-pyran-2-yl)oxy)ethoxy)pyridin-4-yl)aniline (8.8 g, 19.15 mmol, 72% yield). LCMS (m/z) (M+H)= 414.1, Rt = 0.73 min.

A solution of 4-methyl-3-(2-morpholino-6-(2-((tetrahydro-2H-pyran-2-yl)oxy)ethoxy)pyridin-4-yl)aniline (6.39 g, 13.91 mmol), 2-(trifluoromethyl)isonicotinic acid (3.19 g, 16.69 mmol), N1-((ethylimino)methylene)-N3,N3-dimethylpropane-1,3-diamine hydrochloride (3.20 g, 16.69 mmol), 3H-[1,2,3]triazolo[4,5-b]pyridin-3-ol hydrate

(2.57 g, 16.69 mmol), and Huenig's base (2.70 g, 20.86 mmol) in DMF (100 mL) was stirred at RT overnight. HCl (2.0 M aqueous solution, 34.75 mL, 69.5 mmol) was then added and the reaction was stirred for 90 min, at which point LC/MS indicated about 90% conversion to product. Additional HCl (34.75 mL, 69.5 mmol) was added and the mixture stirred for 30 min at RT. The solution was diluted with water and solid sodium bicarbonate was carefully added until pH=5 was reached. The solution was extracted three times with ethyl acetate, and the combined organics were dried over magnesium sulfate, filtered and concentrated. The crude material was purified purified by flash column chromatography over silica gel, eluting with 0-100% ethyl acetate in heptanes, to give N-(3-(2-(2-hydroxyethoxy)-6-morpholinopyridin-4-yl)-4-methylphenyl)-2-(trifluoromethyl)isonicotinamide (6.64 g, 13.08 mmol, 94% yield).

Biochemical Kinase Specificity Profile of 15.

The kinase specificity profile for compound **15** reported in Figure 7 was determined as previously described.[17-18] Compound **15** was assessed in the DiscoverX KINOME*scan* binding assay at 1 μM with activity presented as % of control = [(test compound signal − positive control signal)/(negative control signal − positive control signal]] × 100. Data for the 457 kinase KINOME*scan* are in Supporting Information.

In vivo PK/PD and efficacy

Rat studies were undertaken in accordance with the Novartis Institutes for Biomedical Research Animal Care and Use Committee protocols and regulations. Mice were housed in a temperature- and humidity-controlled animal facility with *ad libitum* access to food and water and acclimated for at least 3 days before experimental procedures.

Crystallography Methods

The crystallization and data collection of wild-type BRAF (residues 445-723) were performed as described previously [2]

SUPPORTING INFORMATION

The Supporting Information is available free of charge on the … for the followings:

Synthetic scheme and experimental procedure of compound **10,** metabolite identification methods, biochemical and cellular assay conditions, X-ray data table for **10** and **15** and unbound fraction of **15** in plasma, molecular formula strings

AUTHOR INFORMATION

Corresponding Author

*E-mail: Savithri.ramurthy@gmail.com. Telephone: **925-324-3692**

ORCID

Savithri Ramurthy: 0000-0002-2444-5309

Notes

The authors declare no competing financial interest.

ACKNOWLEDGEMENTS

We thank Dazhi Tang, Elaine Ginn, Colin Lorentzen, Kent Wong for generating solubility, in vitro ADME data as well as Shengtian Yang for running NMR structural elucidation of **15**.

ABBREVIATIONS USED

Sol, solubility; CP, cell proliferation; Cl, clearance; Vss, volume of distribution; DIEA, diisopropylethylamine; EDC, 1-ethyl-3-(3-dimethylaminopropyl)carbodiimide; HOAt, 1-hydroxy-7-azabenzotriazole; SNAr, nucleophilic aromatic substitution; Rt, retention time; TCEP, (Tris(2-carbosyethyl) phosphine)

REFERENCES

(1) Aversa, R.J.; Barsanti, P.A.; Burger, M.; Dillon, M.P.; Dipsea, A.; Hu, C.; Lou, Y.; Nishiguchi, G.; Pan, Y.; Polyakov, V.; Ramurthy, S.; Rico, A.; Setti, L.; Smith, Aaron.; Subramanian, S.; Taft, B.; Tanner, H.; Wan, L.; Yusuff, N. Biaryl Amide Compounds as Kinase Inhibitors and Their Preparation. WO 2014151616, Sep 25, 2014.

(2) Nishiguchi, G.A.;, Rico,A.; Tanner, H.; Aversa,R.J.; Taft, B. R.; Subramanian,S.; Setti,L.; Burger, M.T.; Wan,L.; Tamez, V.; Smith, A.;Lou, Y.;Barsanti, P.A.; Brent A. Appleton,B.A.; Mamo, M.; Tandeske,L.; Dix,I.; John E. Tellew,J.E.;Huang,S.;. Mathews Griner,L.A.; Cooke,V.G.; Van Abbema,A.; Merritt,H.; Ma,S.; Gampa,K.; Feng,F.; Yuan,J.;Wang,Y.; Haling, J.R.; Vaziri,S.; Hekmat-Nejad,M.; Jansen, J.M.; Polyakov,V.; Zang,R.; Sethuraman,V.; Amiri,P.; Singh,M.;Lees,E.; Shao,W.; Stuart, D.D.; Dillon,M.P.; and Ramurthy, S. Design and discovery of N-(2- methyl-5'-morpholino-6'-((tetrahydro-2H-pyran-4-yl)oxy)-[3,3'-bipyridin]-5yl)-3-(trifluoromethyl) benzamide (RAF709): A potent, selective and efficacious RAF inhibitor targeting RAS mutant cancers. *J. Med. Chem* **2017** *60* (12), 4869-4881

(3) Ostrem, J. M.; Peters, U.; Sos, M.L.; Wells, J.A.; Shokat, K.M. K-Ras(G12C) inhibitors allosterically control GTP affinity and effector interactions. *Nature* **2013**, *503*(7477), 548-551.

(4) Lito, P.; Solomon, M.; Li, L.S.; Hansen, R.; Rosen, N. Allele-specific inhibitors inactivate mutant KRAS G12C by a trapping mechanism. *Science* **2016**, *351*(6273), 604-608.

(5) Patricelli, M.P.; Janes, M.R.; Li, L.S.; Hansen, R.; Peters, U.; Kessler, L.V.; Chen, Y.; Kucharski, J.M.; Feng, J.; Ely, T.; Chen, J.H.; Firdaus, S.J.; Babbar, A.; Ren, P.; Liu, Y. Selective inhibition of oncogenic KRAS output with small molecules targeting the inactive state. *Cancer Discov*. **2016** Mar;*6*(3), 316-329

(6) Hatzivassiliou, G.; Song, K.; Yen, I.; Brandhuber, B. J.; Anderson, D. J.; Alvarado, R.; Ludlam, M. J.; Stokoe, D.; Gloor, S. L.; Vigers, G.; Morales, T.; Aliagas, I.; Liu, B.; Sideris, S.; Hoeflich, K. P.; Jaiswal, B. S.; Seshagiri, S.; Koeppen, H.; Belvin, M.; Friedman, L. S.; Malek, S. RAF inhibitors prime wild-type RAF to activate the MAPK pathway and enhance growth. *Nature* **2010**, 464 (7287), 431−435

(7) Heidorn, S. J.; Milagre, C.; Whittaker, S.; Nourry, A.; NiculescuDuvas, I.; Dhomen, N.; Hussain, J.; Reis-Filho, J. S.; Springer, C. J.; Pritchard, C.; Marais, R. Kinase-dead BRAF and oncogenic RAS cooperate to drive tumor progression through CRAF. *Cell* **2010**, 140 (2), 209−221

(8) Poulikakos, P.I, Zhang, C, Gideon Bollag, G, Shokat, K.M & Rosen. NRAF inhibitors transactivate RAF dimers and ERK signaling in cells with wild-type BRAF *Cell* **2010** 464 427-431

(9) Hauschild,A.; Grob,J.;,L.V.; Jouary,T.; Gutzmer,R.; Millward,M.; Rutkowski,P.; Blank,C.U.;Miller Jr,W.H.; Kaempgen,E.; Martín-Algarra,S.; Karaszewska,B.; Mauch,C.; Chiarion-Sileni,V.; Martin, A.;Swann,S.; Haney,P.; Mirakhur,B.;Guckert,M.E.; Goodman,V.; Chapman, P.B Dabrafenib in BRAF-mutated metastatic melanoma:a multicentre, open-label, phase 3 randomised controlled trial *Lancet* **2012**; 380: 358–365

(10) Karoulia,Z., Yang Wu, Y., Ahmed, T.A., Amaia Lujambio, A.,Gavathiotis,E., Poulikakos, P.I, An Integrated model of RAF Inhibitor action predicts inhibitor activity against oncogenic BRAF signaling. *Cancer Cell* **2016** 30, 485–498

(11) Peng, S.B.; Henry J.R.; Kaufman, M.D.; Lu, W.P.; Smith, B.D.; Vogeti, S.; Rutkoski, T.J.; Wise, S.; Chun, L.; Zhang.; Van Horn, R.D.; Yin, T.; Zhang, X.; Yadav, V.; Chen, S.H.; Gong, X.; Ma, X.; Webster, Y.; Buchanan, S.; Mochalkin, I.; Huber, L.; Kays, L.; Donoho, G.P.; Walgren, J.; McCann, D.; Patel, P.; Conti, I.; Plowman, G.D.; Starling, J.J.; Flynn, D.L. Inhibition of RAF isoforms and active dimers by LY3009120 leads to anti-tumor activities in RAS or BRAF mutant cancers. *Cancer Cell* **2015**, Sep 14; *28*(3), 384-398.

(12) Molecular structure and synthesis of compound **10**, xray co-crystal structure data table of **10** and **15** and kinase profile of **15** are given in the supporting information

(13) Zimmerlin, A; Trunzer M.;, Faller, B. CYP3A time-dependent inhibition risk assessment validated with 400 reference drugs. *Drug Metabolism and Disposition* **2011**, Feb, 39(6), 1039-1046

(14) Vijayan, R.S.K.; He. P.; Modi. V.; Krisna, C.; Duong-Ly.; Ma. H.; Peterson, J.R.; Dunbrack, R.L.; Levy, R.M. Conformational analysis of the DFG-out kinase motif and biochemical profiling of structurally validated Type II inhibitors. *J. Med Chem*. **2015**, *58*, 466-479.

(15) Shao, W.; Mishina, Y. M.; Feng, Y.; Caponigro, G.; Cooke, V. G.; Rivera, S.; Wang, Y.; Shen, F.; Korn, J. M.; Mathews Griner, L. A.; Nishiguchi, G.; Rico, A.; Tellew, J.; Haling, J. R.; Aversa, R.; Polyakov, V.; Zang, R.; Hekmat-Nejad, M.; Amiri, P.; Singh, M.; Keen, N.; Dillon, M. P.; Lees, E.; Ramurthy, S.; Sellers, W. R.; Stuart, D. Unpublished results.

(16) Shao, W.; Mishina, Y. M.; Feng, Y.; Caponigro, G.; Cooke, V. G.; Rivera, S.; Wang, Y.; Shen, F.; Korn, J. M.; Mathews Griner, L. A.; Nishiguchi, G.; Rico, A.; Tellew, J.; Haling, J. R.; Aversa, R.; Polyakov, V.; Zang, R.; Hekmat-Nejad, M.; Amiri, P.; Singh, M.; Keen, N.; Dillon, M. P.; Lees, E.; Ramurthy, S.; Sellers, W. R.; Stuart, D. D. Antitumor properties of RAF709, a highly selective and potent inhibitor of RAF kinase dimers, in tumors driven by mutant RAS or BRAF. *Cancer Res* **2018**, Mar 15; 78(6), 1537-1548

(17) Fabian, M. A.; Biggs III, W. H.; Treiber, D. K.; Atteridge, C. E.; Azimioara, M. D.; Benedetti, M. G.; Carter, T. A.; Ciceri, P.; Edeen, P. T.; Floyd, M.; Ford, J. M.; Galvin, M.; Gerlach, J. L.; Grotzfeld, R. M.; Herrgard, S.; Insko, D. E.; Insko, M. A.; Lai, A. G.; Lelias, J-M.; Mehta, S.A.; Milanov, Z. V.; Velasco, A.M.; Wodcka, L.M.; Patel, H.K.; Zarrinkar, P.P.; Lockhart, D.J. A small molecule-kinase interaction map for clinical kinase inhibitors. *Nat. Biotechnol.*, **2005**, *23*, 329-336.

(18) Karaman, M. W.; Herrgard, S.; Treiber, D. K.; Gallant, P.; Atteridge, C. E.; Campbell, B. T.; Chan, K.W.; Ciceri, P.; Davis, M. I.; Edeen, P. T.; Faraoni, R.; Floyd, M.; Hunt, J. P.; Jockhart, D.J.; Milanov, Z. V.; Morrison, M. J.; Pallares, G.; Patel, H.K.; Pritchard, S.; Wodicka, L. M.: Zarrinkar, P. P. A quantitative analysis of kinase inhibitor selectivity. *Nat. Biotechnol.* **2008**, *26*, 127-132.

(19) Flaherty, K.T.; Jeffery R. Infante, J.R.; Adil Daud, A.; Gonzalez, R.; Kefford, R.F.; Sosman, J.; Hamid,O.; Schuchter, L.; Cebon, J.; Ibrahim, N.; Kudchadkar, R.; Burris III, H.A.; Falchook, G.; Algazi, A.; Lewis, K.; Long, G.V.; Puzanov, I.; Lebowitz, P.; Singh, A.; Little, S.; Sun, P.; Allred, A.; Ouellet, D.; Kim, K.B.; Patel, K.; and Jeffrey Weber, J.; Combined BRAF and MEK inhibition in melanoma with BRAF V600 Mutations. *N Engl J Med* **2012**, 367, 1694-1703.

(20) Flaherty, K.T.; Robert,C.; Hersey,P.; Nathan,P.; Garbe C.; Milhem,M.; Demidov, L.V.; Hassel, J.C.; Rutkowski,P.; Mohr, P.; Dummer,R.; Trefzer,U.; Larkin, J.M.G.; Utikal,J.; Dreno,B.; Nyakas,M.; Middleton,M.R.; Becker,J.C.; Casey,M.; Sherman,L.J.; Wu,F.S.; Ouellet, D.; Martin,A.M.; Patel,K.; and Schadendorf,D.; Improved survival with MEK inhibition in BRAF-mutated melanoma. *N Engl J Med* **2012**, 367, 107-114.

(21) Chapman, P.B.;Axel Hauschild,A.; Robert,C.; Haanen,J.B.; Ascierto,P.; Larkin,J.; Dummer,R.; Garbe, C.; Testori,A.; Maio,M.; Hogg,D.; Lorigan,P.; Lebbe,C.; Jouary,T.; Schadendorf,D.; Ribas,A.; O'Day, S,J.; Sosman,J.A.; Kirkwood,J.M.; Eggermont,A.M.M.; Dreno,B.; Nolop,K.; Li, J.; Nelson B.; Hou,J.; Lee, R.J.; Keith T. Flaherty, K.T.; and Grant A. McArthur, G.A.; Improved survival with Vemurafenib in melanoma with BRAF V600E mutation. *N Engl J Med* **2011**, 364, 2507-2516

(22) Fabbro, D. 25 years of small molecular weight kinase inhibitors: potentials and limitations. *Mol. Pharmacol*. **2015**, *87*(5), 766-775.

"Table of Contents graphic."

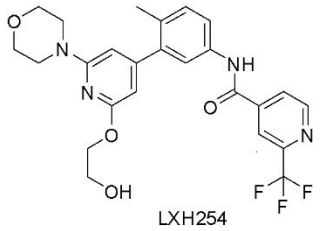

LXH254

pMEK EC_{50} (Calu-6)	0.014 μM
CP EC_{50} (Calu-6)	0.47 μM
Human Mx Cl(int)	13.5 μL/min/mg